THE NATIONAL ACADEMIES PRESS

This PDF is available at http://nap.edu/23263

SHARE

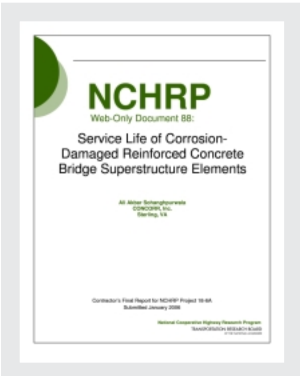

Service Life of Corrosion-Damaged Reinforced Concrete Bridge Superstructure Elements: Web-Only Document

DETAILS

0 pages | null | PAPERBACK
ISBN 978-0-309-42912-2 | DOI 10.17226/23263

AUTHORS

BUY THIS BOOK

FIND RELATED TITLES

Visit the National Academies Press at NAP.edu and login or register to get:

- Access to free PDF downloads of thousands of scientific reports
- 10% off the price of print titles
- Email or social media notifications of new titles related to your interests
- Special offers and discounts

Distribution, posting, or copying of this PDF is strictly prohibited without written permission of the National Academies Press. (Request Permission) Unless otherwise indicated, all materials in this PDF are copyrighted by the National Academy of Sciences.

Copyright © National Academy of Sciences. All rights reserved.

NCHRP

Web-Only Document 88:

Service Life of Corrosion-Damaged Reinforced Concrete Bridge Superstructure Elements

Ali Akbar Sohanghpurwala
CONCORR, Inc.
Sterling, VA

Contractor's Final Report for NCHRP Project 18-6A
Submitted January 2006

National Cooperative Highway Research Program
TRANSPORTATION RESEARCH BOARD
OF THE NATIONAL ACADEMIES

Copyright National Academy of Sciences. All rights reserved.

ACKNOWLEDGMENT

This work was sponsored by the American Association of State Highway and Transportation Officials (AASHTO), in cooperation with the Federal Highway Administration, and was conducted in the National Cooperative Highway Research Program (NCHRP), which is administered by the Transportation Research Board (TRB) of the National Academies.

COPYRIGHT PERMISSION

Authors herein are responsible for the authenticity of their materials and for obtaining written permissions from publishers or persons who own the copyright to any previously published or copyrighted material used herein.

Cooperative Research Programs (CRP) grants permission to reproduce material in this publication for classroom and not-for-profit purposes. Permission is given with the understanding that none of the material will be used to imply TRB, AASHTO, FAA, FHWA, FMCSA, FTA, or Transit Development Corporation endorsement of a particular product, method, or practice. It is expected that those reproducing the material in this document for educational and not-for-profit uses will give appropriate acknowledgment of the source of any reprinted or reproduced material. For other uses of the material, request permission from CRP.

DISCLAIMER

The opinion and conclusions expressed or implied in the report are those of the research agency. They are not necessarily those of the TRB, the National Research Council, AASHTO, or the U.S. Government.

This report has not been edited by TRB.

Copyright National Academy of Sciences. All rights reserved.

THE NATIONAL ACADEMIES

Advisers to the Nation on Science, Engineering, and Medicine

The **National Academy of Sciences** is a private, nonprofit, self-perpetuating society of distinguished scholars engaged in scientific and engineering research, dedicated to the furtherance of science and technology and to their use for the general welfare. On the authority of the charter granted to it by the Congress in 1863, the Academy has a mandate that requires it to advise the federal government on scientific and technical matters. Dr. Ralph J. Cicerone is president of the National Academy of Sciences.

The **National Academy of Engineering** was established in 1964, under the charter of the National Academy of Sciences, as a parallel organization of outstanding engineers. It is autonomous in its administration and in the selection of its members, sharing with the National Academy of Sciences the responsibility for advising the federal government. The National Academy of Engineering also sponsors engineering programs aimed at meeting national needs, encourages education and research, and recognizes the superior achievements of engineers. Dr. William A. Wulf is president of the National Academy of Engineering.

The **Institute of Medicine** was established in 1970 by the National Academy of Sciences to secure the services of eminent members of appropriate professions in the examination of policy matters pertaining to the health of the public. The Institute acts under the responsibility given to the National Academy of Sciences by its congressional charter to be an adviser to the federal government and, on its own initiative, to identify issues of medical care, research, and education. Dr. Harvey V. Fineberg is president of the Institute of Medicine.

The **National Research Council** was organized by the National Academy of Sciences in 1916 to associate the broad community of science and technology with the Academy's purposes of furthering knowledge and advising the federal government. Functioning in accordance with general policies determined by the Academy, the Council has become the principal operating agency of both the National Academy of Sciences and the National Academy of Engineering in providing services to the government, the public, and the scientific and engineering communities. The Council is administered jointly by both the Academies and the Institute of Medicine. Dr. Ralph J. Cicerone and Dr. William A. Wulf are chair and vice chair, respectively, of the National Research Council.

The **Transportation Research Board** is a division of the National Research Council, which serves the National Academy of Sciences and the National Academy of Engineering. The Board's mission is to promote innovation and progress in transportation through research. In an objective and interdisciplinary setting, the Board facilitates the sharing of information on transportation practice and policy by researchers and practitioners; stimulates research and offers research management services that promote technical excellence; provides expert advice on transportation policy and programs; and disseminates research results broadly and encourages their implementation. The Board's varied activities annually engage more than 5,000 engineers, scientists, and other transportation researchers and practitioners from the public and private sectors and academia, all of whom contribute their expertise in the public interest. The program is supported by state transportation departments, federal agencies including the component administrations of the U.S. Department of Transportation, and other organizations and individuals interested in the development of transportation.
www.TRB.org

www.national-academies.org

Copyright National Academy of Sciences. All rights reserved.

TABLE OF CONTENTS

Copyright National Academy of Sciences. All rights reserved.

ACKNOWLEDGMENTS

The work reported herein was performed under NCHRP Project 18-06A by CONCORR, Inc. The principal investigator and author of this report is Ali Akbar Sohanghpurwala, principal of CONCORR, Inc.

The author expresses his sincere gratitude to Dr. John P. Broomfield, Consulting Corrosion Engineer, UK who assisted in preparing a section of the manual and provided field data for use in the project, Dr. Amara Loulizi of Virginia Polytechnic Institute, Blacksburg, Virginia who assisted in the delineation of the climatic zones, Dr. Brian Deifenderfer, formerly an employee of CONCORR, Inc. who is presently employed by The Virginia Research Council, for his assistance in the preparation of the manual, and Dr. Charles C. Antle, Professor Emeritus of Statistics, The Pennsylvania State University, who assisted with the statistical analysis of the data and the validation of the model.

Copyright National Academy of Sciences. All rights reserved.

ABSTRACT

The primary product of this effort was the development of a manual titled “Manual on Service Life Prediction of Corrosion-Damaged Reinforced Concrete Bridge Superstructure Elements.” This manual provides a protocol for assessing the condition of reinforced concrete bridge superstructure elements subjected to corrosion-induced deterioration, predicting the remaining service life of such elements using the developed service life model, and quantifying service life extension for such elements expected from alternative maintenance and repair options. This report documents the data utilized in the development and validation of the service life model presented in the manual.

Copyright National Academy of Sciences. All rights reserved.

INTRODUCTION

Corrosion-induced deterioration of reinforced concrete bridge superstructure elements is a common and recurring problem in the United States. A rational decision regarding maintenance, repair, or replacement of such deteriorated elements must take into account the condition of the element, the extent of deterioration, the expected remaining service life, and the impact of alternative maintenance and repair options on service life of such elements. However, available publications do not provide reliable procedures for evaluating the existing condition of corrosion-damaged elements or approaches for comparing the effectiveness of maintenance and repair alternatives. Without such information, the process of selecting the optimum repair strategy becomes difficult.

Thus, a need was felt for the development of suitable procedures for assessing the condition of corrosion-damaged bridge elements, estimating the expected remaining service life of such elements, and determining the effects of maintenance and repair options on their service life. To meet this need, The National Cooperative Highway Research Program (NCHRP) initiated a project titled “NCHRP 18-06A - Service Life of Corrosion-Damaged Reinforced Concrete Superstructure Elements.”

The objective of this project was to develop a manual, for consideration and adoption by AASHTO, that provides step-by-step procedures for:

1. Assessing the condition of reinforced concrete bridge superstructure elements subjected to corrosion-induced deterioration.

2. Predicting the remaining service life of such elements.

Copyright National Academy of Sciences. All rights reserved.

3. Quantifying service life extension for such elements expected from alternative maintenance and repair options.

This effort was limited to concrete bridge superstructure elements reinforced with epoxy-coated and/or "black" reinforcing steel. It resulted in the development of a manual, available as a separate document, titled "Manual on Service Life Prediction of Corrosion-Damaged Reinforced Concrete Bridge Superstructure Elements" [1]. The first five chapters of the manual discuss the state-of-the-art and lays out the logic for the proposed protocols for condition assessment, predicting remaining service life, and, to some degree, quantifying the service life extension when certain alternatives are utilized in the repair and rehabilitation of bridge superstructure elements. The remaining three chapters of the manual provide step-by-step procedures for implementing the protocols developed in the first six chapters.

The protocol for condition assessment developed in this effort is integrated into the requirements of the National Bridge Inspection Standards (NBIS), thereby, making the implementation of the protocol easier for local, state, and federal agencies. The requirements of condition assessment have been kept to a minimum, recognizing the scarcity of resources that plague almost all governmental agencies. A well defined procedure is proposed which would allow the owner agencies to perform minimal assessment to obtain sufficient information on their bridge superstructure elements and plan the allocation of their resources.

A mathematical model was developed for the initiation of corrosion on both black and epoxy coated rebars. This model allows the user to estimate past progression of damage and project the development of future damage in terms of percent damage of the surface area under consideration. This allows each user to develop the criteria for end of service life that suits their

Copyright National Academy of Sciences. All rights reserved.

needs. A copy of the code (a macro in a spreadsheet) developed specifically to validate the model during the project is also made available with the manual for the users. This macro was not designed for public distribution and may not be as user friendly as desired. A certain degree of familiarity of using a spreadsheet program is required to use this macro.

Based on a literature survey, an attempt was made to provide some guidance with respect to additional service life that may be attainable using various corrosion control, repair, and rehabilitation techniques. Sufficient information from independent sources is not available to provide a conclusive figure for additional service life for many of the technologies discussed in the manual. Additional service life attainable with any corrosion control or repair and rehabilitation technique is dependent on many factors, the most important of which is the applicability of that particular technique to the subject structure based on its corrosion condition, presence of other deterioration processes, and the exposure environment. In addition, the quality of the design and the application of the technique also significantly impact their performance.

The mathematical model developed in this effort was validated against 3 bridge structures located in varying environments in the United States of America. Two evaluations, two years apart, were conducted to ascertain the condition of the structure. The results of the first evaluation were used to model the corrosion process and to calibrate the model and the second evaluation was used to validate the ability of the model to project future deterioration. This report documents the data collected, analysis of the data, and the validation of the model.

Copyright National Academy of Sciences. All rights reserved.

RESEARCH APPROACH

Definition of Service Life

At the initiation of the project, the research team attempted to define the criteria for the end of service life for use in this effort. Review of literature indicated that various different definitions of service life were in use and each was appropriate for a certain group of concrete structures in a certain environment and for a given application. For example, some researchers defined end of service life to be when the first corrosion induced crack occurred, others defined it to be when 20 percent of the concrete surface had suffered corrosion induced damage, and still others used several more criterion for definition of end of service life. Therefore, the definition of the end of service life was left to the user and the service life model was designed to output the deterioration of concrete as a function of time. Each user could use this information along with an appropriate definition of end of service life. It should be noted that all reference to concrete deterioration in this report is to damage resulting from corrosion of embedded reinforcement.

Development of Exposure Zones

To accomplish one of the goals of the project, develop a service life model applicable to bridge superstructure elements exposed to varying degrees of corrosivity, it was necessary that the model be validated on various structures located in varying corrosive environments. The measure of corrosivity of an environment includes the level of exposure to chloride ions, moisture, and temperature. Chloride ions are essential for the breakdown of passivity and the initiation of corrosion. Moisture is necessary for the continuation of the electrochemical process, and temperature (in addition to other factors) impacts the rate of the reaction.

Copyright National Academy of Sciences. All rights reserved.

As no index is available to quantify the level of corrosivity, average annual snowfall, number of days per year with snow in excess of 1 inch on the ground, salt usage per lane per mile, and mean annual temperature can be used to qualitatively define the corrosivity of a region. To overcome the logistics of verifying the model on each micro climatic and exposure condition, an alternative solution was selected. The alternative solution included subdividing the country into 6 zones representative of the variation in corrosivity. Figure 1 depicts the subdivision of the country into 6 zones developed for this project. The delineation of zones was based on climatic conditions

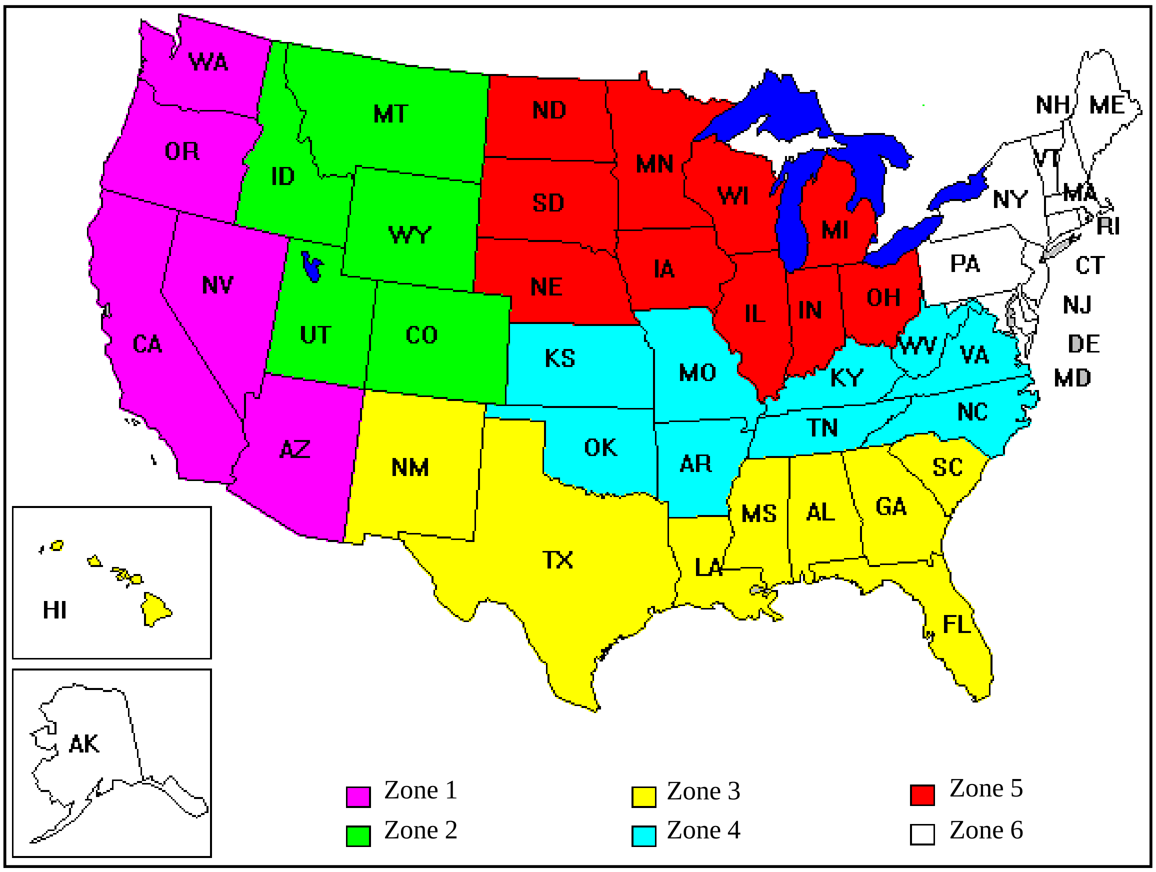

Figure 1: Delineation of zones based on corrosivity of the exposure conditions.

and the use of deicing salts. Mean annual snowfall, mean number of days per year with 1 inch of snow on the ground, salt usage, and mean annual temperature were the parameters used to

Copyright National Academy of Sciences. All rights reserved.

develop the exposure zones. Delineation of the country into various environmental or corrosive zones by other authors was also considered.

Annual Snowfall

Although it would be preferable to have somewhat uniform snowfall within a zone, it is almost impossible to accomplish. Most of the zones show reasonable uniformity with the exception of Zones 1, 2 and 6 as shown in Figure 2. Annual snowfall in Zone 1 varies from 1 inch to 197 inches and the number days per year with 1 inch or more of snow varies from the lowest range of 1 to 5 days to over 100 days.

Zone 2 exhibits less variation than Zone 1, but significantly higher than the other zones. The mean annual snowfall ranges from 15 inches to greater than 98 inches. The number of days with 1 inch or more of snow on the ground for this region is somewhat constant and exceeds 50 days per year. Snowfall in Zone 6 varies from 59 inches to 197 inches.

The other three regions have a more uniform distribution of annual snowfall. The variation of the mean annual snowfall for the remaining zones is as follows:

- Zone 3 less than 5 inches (except for the State of New Mexico)
- Zone 4 ranges from 5 to 30 inches
- Zone 5 ranges from 15 to 59 inches.

The Transportation Research Board (TRB) divides the US into 9 regions: Pacific West, Mountain, Upper Plains, Lower Plains, Great Lakes, New England, Upper Middle Atlantic, Lower Middle Atlantic, and South, as shown in Figure 3 [2].

Copyright National Academy of Sciences. All rights reserved.

Due to uniformity in the annual snowfall, six of the TRB regions were reduced to three by combining the Lower Plains states and the Lower Middle Atlantic states to form Zone 4, the Upper Plains states and the Great Lakes states to form Zone 5, the New England states and the Upper Middle Atlantic states to form Zone 6. In addition, the state of New Mexico was moved from the mountain regions to be part of Zone 3 since this state has many regions with mean annual snowfall of less than 30 inches.

The Longterm Pavement Program (LTPP) subdivided the country into four environmental regions: Wet-Freeze, Wet-Nonfreeze, Dry-Freeze, and Dry-Nonfreeze as shown in Figure 4. With the exception of Zone 2, all zones developed for this study encompass more than one LTPP environmental region.

Temperature

The mean daily average temperature variation throughout the country is presented in Figure 5. Zone 1 exhibits the largest variation in temperature varying from less than 32°F to over 70°F, Zones 2, 5, and 6 exhibit a more modest variation in temperature, Zone 4 exhibits the least variation, and Zone 3 is the warmest.

Copyright National Academy of Sciences. All rights reserved.

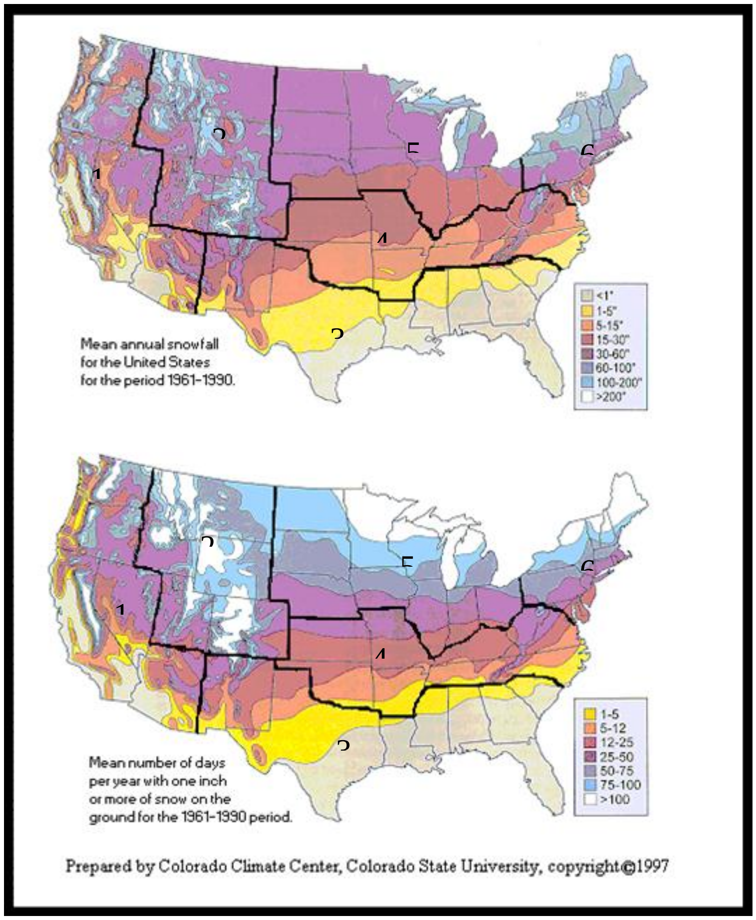

Figure 2: Mean annual snowfall and mean number of days per year with 1 inch or more of snow on the ground in the US.

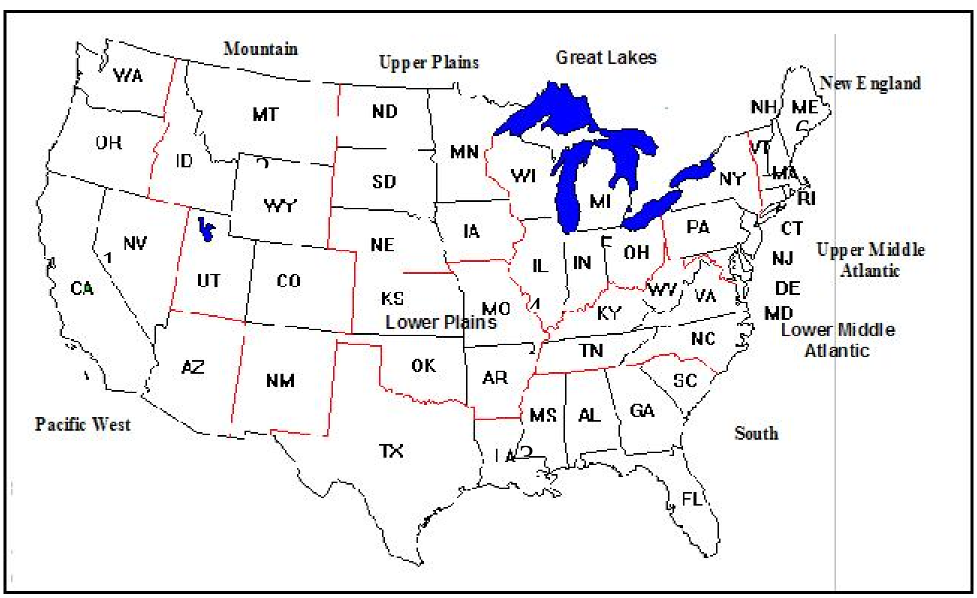

Figure 3: US climatic regions as defined by Transportation Research Board.

Copyright National Academy of Sciences. All rights reserved.

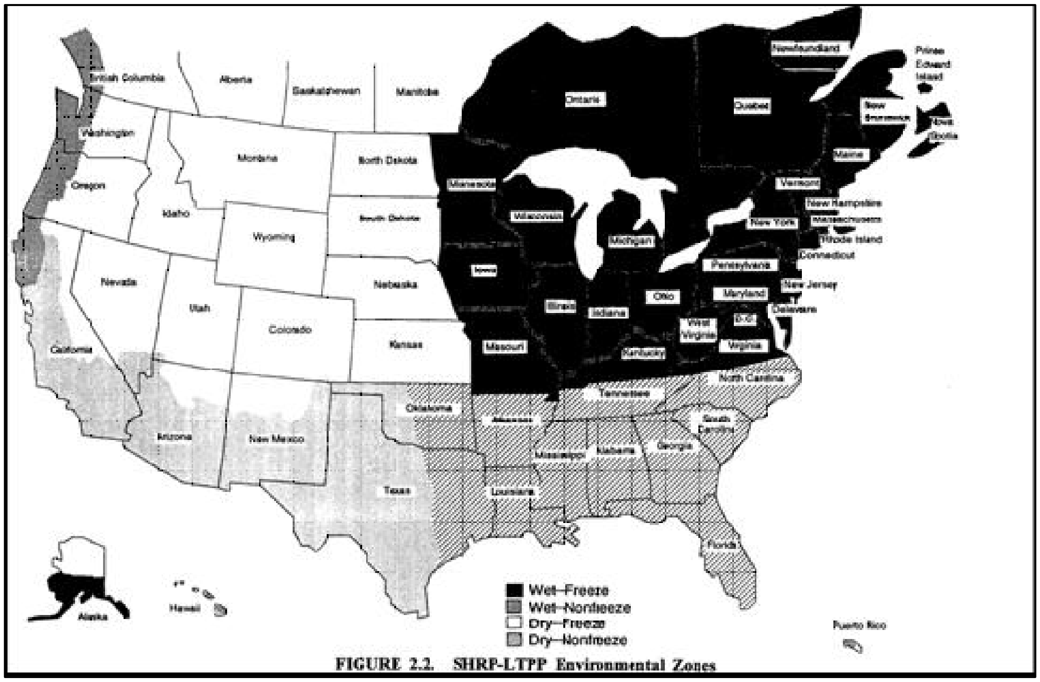

Figure 4: Climatic regions as defined by the Longterm Pavement Program.

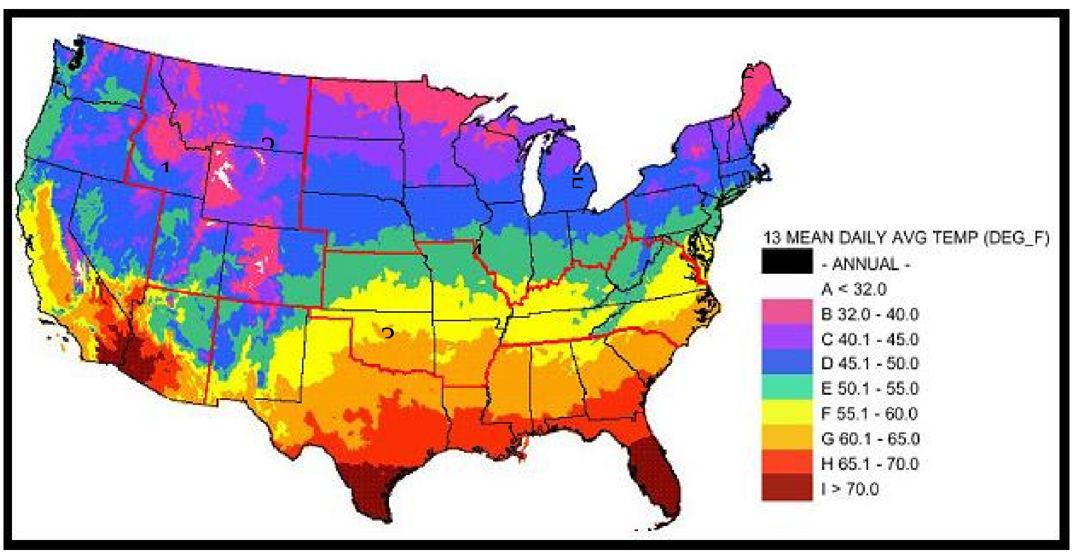

Figure 5: Mean daily average temperature.

Copyright National Academy of Sciences. All rights reserved.

Salt Usage

In 1991, TRB developed the distribution of road salt usage (roads and bridges) as shown in Figure 6 for the 9 regions discussed above [2].

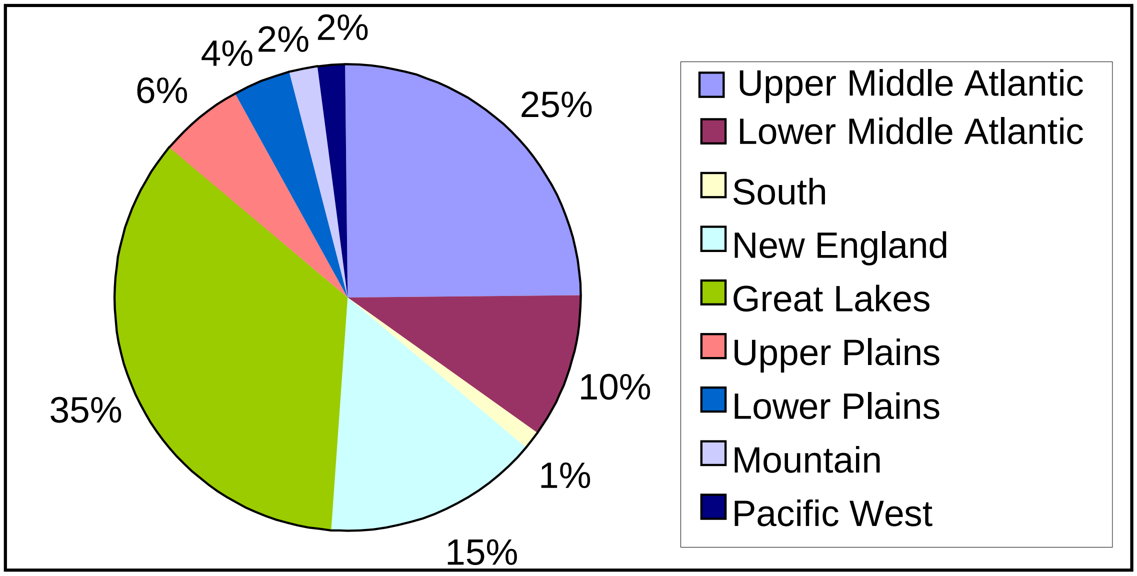

Figure 6: Salt use by regions.

The majority of the salt is used by states in the New England, Great Lakes, and Middle Atlantic Regions (85%). States in the Plains and Mountain regions use only 14% of the total salt as they have lighter traffic demand and longer periods of cold temperature. The states in these two regions rely mainly on sanding and plowing for snow and ice control [2]. A look at the average annual salt loading reveals the same conclusion; the aforementioned three regions apply more salt per lane mile (Table 1).

Copyright National Academy of Sciences. All rights reserved.

Table 1: Salt Usage by State

Region and State	Average Annual Loading Tons/lane-mile	Region and State	Average Annual Loading Tons/lane-mile
Middle Atlantic		**Plains**	
Delaware	9	Iowa	3.8
Maryland	7.1	Minnesota	5
New Jersey	6.7	Missouri	1
New York	16.6	Nebraska	1.5
Virginia	3	Oklahoma	1.5
West Virginia	6.3	South Dakota	1
Great Lakes		**Mountain and West**	
Illinois	6.6	Alaska	1.2
Indiana	9	California	3
Michigan	12.9	Idaho	0.3
Ohio	9.1	Nevada	1.9
Wisconsin	9.2	New Mexico	0.5
New England			
Maine	8		
Massachusetts	19.4		
New Hampshire	16.4		
Vermont	17.1		

Based on Figure 6, the distribution of salt usage in the 6 Zones defined in this study is as follows:

Zone 1	2%
Zone 2	2%
Zone 3	1%
Zone 4	15%
Zone 5	41%
Zone 6	40%

Thus, Zones 1 to 3 form the low usage regions, Zone 4 the medium usage region, and Zones 5 and 6 the high usage regions.

Copyright National Academy of Sciences. All rights reserved.

Corrosivity

Corrosivity for reinforced concrete structures is directly related to salt exposure, either from deicing or marine salts. A study performed in 1985 developed a map (see Figure 7) of the US exhibiting variation in corrosivity throughout the country [3]. This measure of corrosivity also included the reduction in pH due to acid rain. Figure 7 identifies Zone 6 to be a severe environment, Zone 5 to vary from mild to severe, coastal regions of Zones 1 to 3 to vary from moderate to severe, and Zone 4 to be negligible.

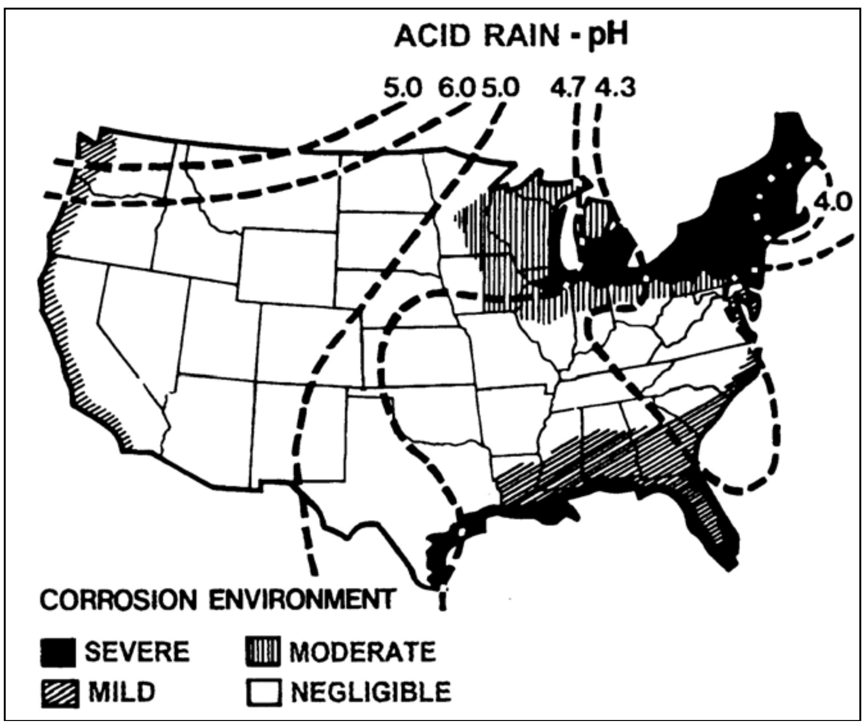

Figure 7: Corrosion environment of the US

With the exception of the coastlines of Zones 1, and 3, and the entire Zone 4, the corrosivity of all other areas of the country match well with the salt consumption discussed above. The coastlines are quite understandable as marine salts impact them. A study by the Oregon Department of Transportation has shown that distance from the ocean has a very significant

Copyright National Academy of Sciences. All rights reserved.

effect on the corrosion rate of mild steel[4]. The low corrosivity of Zone 4 in this map is in contrast to corrosivity expected from the magnitude of salt usage.

Selection of Bridge Structures for Validation

To validate the model developed in this program, one bridge from each of the above developed exposure zones was selected. Due to budget limitations, it was decided that only bridge structures using black reinforcing steel in the construction of the bridge deck would be included in the study. However, the selected structures needed to meet a set of criteria to be useful to this effort. A request was sent out to each and every State in the 48 contiguous states in the United Sates of America to identify two to three bridge structures in their states that met the following criteria:

Present Condition:	The structure must be suffering from corrosion induced damage or is likely to suffer such damage in the near future.
Past Repairs:	It is preferable that the bridge deck has not undergone any repairs to date. Patching of small damaged areas by maintenance crews is not considered repair for the purpose of this project.
Bridge deck:	The bridge deck should be conventionally reinforced and not have an asphalt overlay and/or waterproofing membrane.
Length of the deck:	The bridge deck should be in excess of 80 feet in length.
Age:	The age of the structure should be in excess of 20 years.

and to provide requested information about these structures. A total of 19 states responded to the

Copyright National Academy of Sciences. All rights reserved.

project team's request. At least one state had responded from each of the 6 exposure zones. The received information was analyzed and 6 structures were selected for validation. The selected structures are listed in Table 2. With the exception of the structure in Maryland, all other structures were about the same age, constructed between 1968 and 1973, whereas the Maryland structure was constructed in 1934.

Field Evaluation

A total of two evaluations were performed on the bridge decks of each of the selected bridges with the exception of the structure located in the State of Colorado where only one field evaluation was performed. The two evaluations were performed approximately 2 years apart. Although, a much longer gap (5 to 7 years) between the field evaluations was desirable, the time constraint of the project allowed the maximum of 2 years.

The first evaluation was conducted between the months of July and September of 2002. One lane from each of the bridge decks was selected for evaluation and the following tests were performed:

1. Delamination Survey
2. Core Sample Collection
3. Clear Concrete Cover Survey
4. Corrosion Rate Measurements

Copyright National Academy of Sciences. All rights reserved.

Copyright National Academy of Sciences. All rights reserved.

Table 2: Bridge structures selected for field validation study.

	California	Colorado	New Mexico	Kentucky	Ohio	Maryland
Located in Zone	1	2	3	4	5	6
Bridge ID	41C0012	E-16-CW	7028	B3	JEF00220078	100091001
County	Maderas	Denver	Socorro	Woodford	Jefferson	Brunswick
Road Carried	Santa Fe Blvd	Tabor St	SB I-25	Route 341	Beacon Ridge Rd	MD Route 464
Going Over	Berenda Slough	I-70	Manzaneras St	I-64	Route 22	Catoctin Creek
Year Constructed	1968	1971	1970	1973	1969	1934
Number of Spans	6	2	3	4	4	4
Average Daily Traffic	259	n/a	4375/4600	1341	n/a	3050
Dimension of the Lane Surveyed	182' x 16'	222' x 14' 9"	108' 7" x 21' 8"	276' 4" x 23' 10"	204' x 12' 6"	305' x 10' 6"
Direction of Traffic	Northbound	Southbound	Southbound	Northbound	Northbound	Northbound
First Evaluation	August-02	August-02	September-02	September-02	September-02	July-02
Second Evaluation	September-04	n/a	September-04	June-04	June-04	June-04

The delamination survey was conducted first over the entire surface area of the test lane using standard sounding techniques. This was followed by the collection of cores from select areas. The collection of the cores was performed in a pattern such that the variation of surface chloride ions as a function of distance along the width of the lane can be analyzed. The coring schedule required that 50 percent of the cores be collected from the right edge of the lane, 25 percent from the center of the lane, and 25 percent from the left edge of the lane. Therefore, at every odd numbered coring location, one core from the right edge of the lane was collected and at every even numbered coring location three cores were collected. Cores were not collected from delaminated or patched areas. The presence of delamination and lack of access to one edge of the lane due to safety concerns in some instances disrupted this core collection scheme. On all bridge decks a minimum of 33 cores were collected. However, some of the cores disintegrated, failed along cracks, or were damaged and therefore could not be used for chloride profile analysis. The cores were collected with a 2 inch diameter core bit by coring down 5 inches into the deck. The goal was to obtain a core at least 4 inches long. A total of 215 cores were collected during the first evaluation from the 6 bridge decks. Clear concrete cover measurements were made at various locations using a covermeter. The covermeter measurements were compared to actual cover at select locations. Finally, corrosion rate measurements were performed adjacent to the sites where cores were collected. The measurement was performed on a reinforcing bar that was located closest to the core site. In several instances, the project team experienced problems with the measurement and the corrosion rate measurements could not be made. In some cases the problems with the measurement were attributable to the malfunctioning of the corrosion rate device and in other cases the corrosion rate was too low to be measured. The corrosion rate measurements were performed using the three electrode linear polarization

Copyright National Academy of Sciences. All rights reserved.

technique with the Gecorr 6 device.

The second evaluation was conducted from June to September, 2004 and the following tests were performed in the same lane that was selected in the first evaluation for 5 bridge decks:

1. Delamination Survey
2. Half-cell Potential Survey
3. Corrosion Rate measurements
4. Core Sample Collection

An evaluation of the bridge located in the State of Colorado could not be performed due to logistical and scheduling problems.

The delamination survey was performed in the same manner it was performed in the first evaluation. The Half-cell potential survey was performed over the entire surface of the selected lane and corrosion rate measurements were only performed at selection locations exhibiting the most negative half-cell potential. Fewer cores were collected for profile analysis. A total of 16 cores were collected from 5 bridge decks.

Laboratory Evaluation

The cores collected in the field were analyzed for chloride concentration at various depths. From each core, powdered concrete samples were collected from defined depths. A 4 inch section of each core was subdivided into slices 0.4 inches (10 mm) thick by marking its boundaries on the side of the core. A maximum of 10 powdered samples were obtained from each core. A

Copyright National Academy of Sciences. All rights reserved.

diamond based abrasion disk was used to powder the slices sequentially. The powdered samples were analyzed for total chloride ion content in accordance with the AASHTO-T-260-94 "Sampling and Testing for Chloride Ion in Concrete and Concrete Raw Materials." The concentrations of the chloride ions at various depths for each core were plotted and the diffusion coefficient was calculated for each core.

Model Development

A mathematical model was developed for both black and epoxy coated reinforcing steel. The details of this model are discussed in the manual. A macro was written in a spreadsheet program to compare the model results against the results obtained from the field. The macro is also available along with the manual. The model for epoxy coated rebar was not validated as sufficient information was not found in a literature review.

Copyright National Academy of Sciences. All rights reserved.

RESULTS AND DISCUSSION

Chloride Profiles & Clear Concrete Cover

Chloride ion concentrations at various depths from each core were plotted to develop the chloride profile for each core. The diffusion coefficient for each core was estimated by fitting a curve to the profile using non-linear regression analysis. The following curve was fitted to each profile:

$$C_{(x,t)} = C_0\left[1 - erf\left(\frac{x}{2\sqrt{Dt}}\right)\right]$$

by minimizing the sum of squares of the vertical distance between the actual data and the selected curve. A typical curve fit is provided in Figure 8. For some cores, the chloride ion

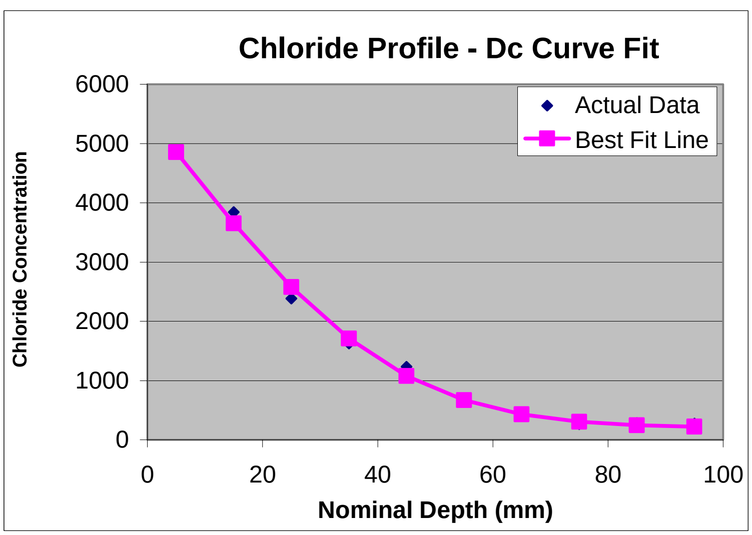

Figure 8: Curve Fit to ascertain "Apparent Diffusion Coefficient."

distribution in the cores did not exhibit diffusion characteristics and they had to be eliminated from the analysis. The cores from the bridge structure located in the State of California

Copyright National Academy of Sciences. All rights reserved.

exhibited redistribution of chloride ions in the concrete and a decrease in chloride ion concentration in the top several inches. It was later learned that the State of California Department of Transportation had stopped applying salt on the structure some time ago and therefore the chloride ions present in the concrete were simply diffusing down the deck with the surface chloride concentration decreasing with time. Therefore the data from the state of California was not used for model validation.

The chloride ion concentration at the 0 to 0.4 inches (0 to 10 mm) depth of each core was considered to be the surface chloride ion concentration at that location. In many instances, it was observed that the chloride ion concentration in the first 0.4 inches (10 mm) depth was variable and less than the concentration at the second 0.4 inches (10 mm) depth (0.4 inches to 0.8 inches (10 mm to 20 mm)). Per the diffusion equation, the surface concentration is the driving force and should be larger in magnitude than the chloride ion concentration at any other depth. This anomaly can be explained by the effect of exposure of the top layer of concrete to moisture that can wash away a portion of the surface chloride ions. Therefore, in instances where the concentration of chloride ions in the 0 to 0.4 inches (10 mm) depth was less than the 0.4 inches to 0.4 inches (10 mm to 20 mm) depth, the concentration at the 0.4 inches to 0.8 inches (10 mm to 20 mm) depth was used as the surface chloride ion concentration or the driving force in the diffusion equation. In some cores, the concentration from a nominal depth deeper than 0.6 inches (15 mm) had to be used as surface chloride ion concentration.

The clear concrete cover information obtained using the cover meter was used in the analysis. Tables A-1 to A-5 and Figures A-1 to A-5 in the Appendix list the distribution of calculated diffusion coefficients, surface chloride ion concentrations, and clear concrete cover. In general,

Copyright National Academy of Sciences. All rights reserved.

the surface chloride ion concentration and the clear concrete cover could be best described by a normal distribution curve and the diffusion coefficients were best described by a gamma distribution curve.

Delamination Survey

A delamination survey was conducted on the entire surface of the selected lane using a chain drag. The delaminations were marked on the surface and the size of each delamination was documented along with an approximate location of the delamination. To document the dimensions of the delaminations, the smallest square or a rectangle that could enclose the irregular geometry of the delamination was drawn and its dimensions were documented. A summary of the delamination data is provided in Table 3.

Table 3: Summary of Delaminations Detected

States		NM	OH	KY	MD	CA	CO
Area Surveyed		2353	2550	6586	3227	2913	3275
1st Trip	Delaminated Square feet	723	369	570	2811	1015	1132
	% Delaminated	31%	14%	9%	87%	35%	35%
2nd Trip	Delaminated Square feet	1636	418	751	2858	1036	
	% Delaminated	70%	16%	11%	89%	36%	0%

In the State of New Mexico, the delaminations jumped from 31 percent to 70 percent in two years. Observation on the bridge indicated that not all of the increase in delaminations had resulted from corrosion. The vibration of the deck that was observed every time a large vehicle passed suggests that much of the increase in delamination may have resulted from mechanical

Copyright National Academy of Sciences. All rights reserved.

stress. On one span, the entire deck was delaminated during the second evaluation.

In the State of Maryland, the bridge deck had suffered significant damage and much of the damage had been repaired. The patch repairs were considered to be delaminated for the purpose of this project. Additional delaminations were observed in the original concrete. For expediency, the delamination survey was only performed on the original concrete as more than 60 percent of the deck surface had already been patch repaired.

Corrosion Rate Measurements

During the first trip, corrosion rate measurements were performed, where possible, at every core collection site on a rebar located closest to the core site during the first evaluation. During the second evaluation, the corrosion rates were measured at locations exhibiting the most negative potentials. A summary of the corrosion rate data is provided in Table A-6 in the Appendix. In general, the average corrosion rates in the states of California, New Mexico, Kentucky, and Ohio are in the low range, for Colorado is in the moderate range, and Maryland is in the high range. The corrosion rate measurements were not used in the modeling process and therefore are not discussed further.

Half-cell Potential Measurement

Half-cell potential measurements were collected on a 2 feet grid on each of the deck surfaces during the second evaluation. Half-cell potentials were not obtained from delaminated areas. When a delamination did not encompass the entire 2 feet by 2 feet square of the grid, the half-cell potential was collected from the portion of the square that was sound. The half-cell data is

Copyright National Academy of Sciences. All rights reserved.

presented in Figures A-6 to A-10 in the Appendix using a color code. The half-cell potentials measurements were not used in the modeling process and therefore are not discussed further.

Model Results

The model developed in this project utilizes diffusion coefficients, surface chloride concentration, and clear concrete cover information to estimate the diffusion of the chloride ions into concrete and the time to corrosion initiation. The time to propagation is assumed to be 5 years. The model outputs damage as a function of age from the time of construction to 100 years of age. The model also calculates the Susceptibility Index which provides information on the distribution of the chloride ions at the steel depth as compared to the chloride threshold.

The model was first run using all of the cores collected in the first evaluation for a given structure. This was considered the full sample set for the subject structure. For each structure the chloride threshold was adjusted such that the models' estimate of delaminations at the age the first evaluation was conducted matched with the actual delaminations measured on the deck. Then, the models prediction for the damage at the age of the structure during the second evaluation was compared to the actual delaminations measured during the second evaluation on the structure. This allowed the model to be calibrated to one data point and the second data point was used for judging the accuracy of the model in predicting future damage. The validation on the bridge structure located in the State of Colorado could not be performed as data from a second evaluation was not available. The bridge structure in New Mexico also had to be dropped from the validation studies as a significant portion of the delaminations observed were not considered to have resulted from corrosion of reinforcement and, therefore, the structure was

Copyright National Academy of Sciences. All rights reserved.

not a good candidate for validation. A total of three bridge structures located in the States of Kentucky, Ohio, and Maryland were used in the validation studies. The output of the model for the full sample set for these three structures is provided in the Appendix.

Once the results, with the full sample for each structure, were obtained, the cores were then randomly subdivided into sets of 5. Each set of 5 cores was considered to be an independent sample set and the model was run using each set of 5 cores as the input. Subsequently, the full set of cores were randomly subdivided into sets of 10, 15, 20 25, 30, and 35 cores when possible and these sample sets were used as independent sample sets. This resulted in a total of 37 sample sets from the three bridge structures included in the study.

The validation studies were run in two different ways. In the first evaluation, the model was run for all sub-sample sets adjusting the chloride threshold to calibrate the output of the model to the delamination survey results of the first evaluation. In the second study, the chloride threshold required for the calibration of the model with the full set of cores for the given structure was used in running the model with other sample sets as input for the model from the same structure. The chloride threshold was not adjusted for these smaller sample sets.

Table 4 presents the results of the first validation study in which the chloride threshold was varied for each set to calibrate the output of the model to the delamination survey results of the first evaluation. The analysis of the prediction for the second evaluation suggests that the maximum error in predicting the damage 2 years from the calibration age does not exceed 4% and the standard deviation does not exceed 1%. This suggests that the model is reasonably accurate in predicting two years out from the age of calibration. It is expected that the error will

Copyright National Academy of Sciences. All rights reserved.

increase with advance in time from the age of the calibration.

The chloride threshold required to calibrate the model ranged from 130 to 955 ppm with an average of 578 ppm and a standard deviation of 201 ppm (see Table 5). The Susceptibility Index as calculated for each sample set did not vary much from that calculated for the full sample at the age of the second evaluation (see Table 6). The average error in the SI (difference in SI between the full sample and the sub-sample) was 1 with a standard deviation of 2. For the two bridge structures located in Kentucky and Ohio there was essentially no difference in SI calculated from the full set or the sub-sample set. Only the structure located in Maryland exhibited some variation. This variation was due to the fact that the ratio of sound concrete remaining on the bridge deck compared to the sum of repaired and delaminated was significantly very low. Therefore, the remaining sound concrete would be represented by the extreme values of cover, surface chloride concentration, and diffusion coefficients.

When the model was run on subsets using a fixed chloride threshold, as determined by the full sample set for that particular structure, the results for the subset exhibited a much larger variation in prediction 2 years from the calibration age (See Table 7). This variation in prediction is the result of the sensitivity of the model to its input. The maximum error was 16 % with a maximum standard deviation of 5 %. The calculation of the Susceptibility Index did not exhibit much variation from set to set (see Table 8). The accuracy of the model in predicting damage in the future is very dependent on the sample used for the input. Small samples, especially those that are not representative of all the conditions in the structure, can result in diffusion coefficients and surface chloride ion content distributions that are very different than the actual distributions for

Copyright National Academy of Sciences. All rights reserved.

Table 4: Predictions at a Variable Chloride Concentration

State	Measured	# of Cores	# of Predictions	Statistics for Predictions				Error in Predictions			
				Min	Max	Average	Standard Deviation	Min	Max	Average	Standard Deviation
MD	89	5	3	87	88	88	1	1	2	1	1
OH	16	5	7	17	19	18	1	1	3	2	1
KY	11	5	7	12	15	13	1	1	4	2	1
OH	16	10	3	18	19	18	1	2	3	2	1
KY	11	10	3	14	14	14	0	3	3	3	0
KY	11	15	2	13	14	14	1	1	3	3	1
ALL		5	15					1	4	2	1
ALL		10	6					2	3	3	1
ALL		ALL	37					0	4	2	1

Table 5: Chloride Threshold at a Variable Chloride Concentration

State	Clth at Full Sample	# of Cores	# of Predictions	Statistics for Chloride Threshold				Error in Chloride Threshold			
				Min	Max	Average	Standard Deviation	Min	Max	Average	Standard Deviation
MD	200	5	3	130	955	562	414	70	755	408	343
OH	725	5	7	495	900	738	159	25	230	129	78
KY	460	5	7	235	710	479	165	35	250	130	89
OH	725	10	3	525	850	700	164	0	200	108	101
KY	460	10	3	390	575	488	93	40	115	75	38
KY	460	15	2	475	500	488	18	18	40	28	18
ALL		5	15	130	955	581	231	25	755	179	185
ALL		10	6	390	850	594	166	0	200	92	71
ALL		ALL	37	130	955	579	201	0	755	115	147

Copyright National Academy of Sciences. All rights reserved.

Table 6: SI at a Variable Chloride Concentration

State	SI for Full Sample	# of Cores	# of Predictions	Statistics for SI				Error in SI			
				Min	Max	Average	Standard Deviation	Min	Max	Average	Standard Deviation
MD	9	5	3	0	6	3	3	3	9	6	3
OH	5	5	7	4	5	5	0	0	1	0	0
KY	6	5	7	5	6	6	0	0	1	0	0
OH	5	10	3	4	5	5	1	0	1	0	1
KY	6	10	3	6	6	6	0	0	0	0	0
KY	6	15	2	5	6	6	1	1	1	1	1
ALL		5	15					0	9	1	3
ALL		10	6					0	1	0	0
ALL		ALL	37					0	9	1	2

Copyright National Academy of Sciences. All rights reserved.

Copyright National Academy of Sciences. All rights reserved.

Table 7: Predictions at a Constant Chloride Concentration

State	Measured	# of Cores	# of Predictions	Statistics for Predictions				Error in Predictions			
				Min	Max	Average	Standard Deviation	Min	Max	Average	Standard Deviation
MD	89	5	3	85	99	94	8	4	10	8	3
OH	16	5	7	6	31	18	9	1	15	8	5
KY	11	5	7	3	27	14	9	1	16	7	5
OH	16	10	3	7	25	16	9	1	9	6	5
KY	11	10	3	9	19	15	5	2	8	5	3
KY	11	15	2	13	17	15	3	3	6	4	3
ALL		5	15					1	16	7	5
ALL		10	6					1	9	6	4
ALL		ALL	37					1	16	5	4

Table 8: Predictions at a Constant Chloride Concentration

State	SI for Full Sample	# of Cores	# of Predictions	Statistics for SI				Error in SI			
				Min	Max	Average	Standard Deviation	Min	Max	Average	Standard Deviation
MD	9	5	3	2	6	4	2	3	7	5	2
OH	5	5	7	3	6	5	1	0	2	1	1
KY	6	5	7	4	8	6	1	0	2	1	1
OH	5	10	3	4	6	5	1	0	1	1	1
KY	6	10	3	6	7	6	1	0	1	0	1
KY	6	15	2	6	6	6	0	0	0	0	0
ALL		5	15					0	7	2	2
ALL		10	6					0	1	1	1
ALL		ALL	37					0	7	1	2

these parameters in the structure. To overcome the sensitivity of the model to the input, we have chosen to vary the chloride threshold. This reduces the model's sensitivity to the sample used as input to the model and calibrates the model to one data point.

Considering the engineering application for which this kind of modeling is used, the accuracy does not have to be very high. A 5% to 10% error is tolerable and in most cases may not significantly impact the repair and rehabilitation decision. The Susceptibility Index fares better and is less sensitive to variation in the input to the model, and is likely to play a significant role in the decision making process.

In addition, a cumulative Weibull distribution curve was fit to the data from the model to determine if such a cumulative distribution could be used in lieu of the modeling. The Weibull distribution curve correlates well with the initial segment of the model results (the first 10 to 30 years of age) and then underreports damage compared to the model results. The model results for all structures with the full set of cores are provided in Figure A-11 of the Appendix.

Conclusions

In general, the model seems to provide reasonable accuracy for the near future when the output of the model is calibrated to know damage at a given age. It is expected that the error in the prediction would increase with the age from which the calibration was made. This is expected as corrosion induced damage increases, other deterioration processes are enhanced and the rate of increase of damage is then governed not only by the rate of the corrosion process.

Copyright National Academy of Sciences. All rights reserved.

The output of the model and the Susceptibility Index together can be a powerful tool that can be wielded in a decision making process to repair and maintain reinforced concrete superstructure elements. This validation process is somewhat limited in that the predictions could only be compared to a time 2 years beyond the calibration age. A 5 or a 10 year time frame for comparison would provide better insight into the accuracy of the model.

Future Research

This effort was significantly focused on the corrosion initiation phase of the corrosion process. It is recommended that future efforts be more focused on the time to propagation. Several researchers have shown that the clear concrete cover does impact the time to propagation and developing and validating the time to propagation phase would significantly improve the model output.

Copyright National Academy of Sciences. All rights reserved.

REFERENCES

1. Sohanghpurwala, A.A., *Manual for Service Life Prediction of Corrosion-Damaged Reinforced Concrete Bridge Superstructure Elements*. 2005, American Association of State and Highway Officials.

2. *Highway Deicing: Comparing Salt and Calcium Magnesium Acetate*, in *Speical Report 235*. 1991, Transportation Research Board: Washington, DC. p. 163.

3. Turcotte, R., and Baboian, R. *Development of Poultice Corrosion Tests for Automobiles*. in *Corrosion 1985*. 1985. Boston, Massachusetts: National Association of Corrosion Engineers.

4. *Evaluation of Rocky Point Viaduct Concrete Beam*. 2000, Oregon Department of Transportation. p. 85.

Copyright National Academy of Sciences. All rights reserved.

APPENDIX

Copyright National Academy of Sciences. All rights reserved.

Table A-1: Core Information for Structure in Colorado

Core ID	Span	X Loc feet	Y Loc feet	Dc mm/year	Co ppm
S1-L1-1R	1	6	4	3	1950
S1-L1-1M	1	5	8	33	3922
S1-L1-2R	1	10	2	21	1243
S1-L1-3R	1	20	3	8	1956
S1-L1-2M	1	18	8	17	2953
S1-L1-2L	1	20	13	47	4303
S1-L1-4R	1	28	4	26	4622
S1-L1-5R	1	36	2	23	2539
S1-L1-6R	1	50	4	13	3892
S1-L1-3M	1	52	8	33	3438
S1-L1-3L	1	54	13	39	3427
S1-L1-8L	1	75	5	149	3196
S2-L1-1R	2	121	4	48	2706
S2-L1-2R	2	132	3	2	1314
S2-L1-3R	2	143	3	177	1206
S2-L1-4R	2	152	2	3	1726
S2-L1-5R	2	157	3	41	2965
S2-L1-1M	2	165	7	22	4231
S2-L1-1L	2	166	13	47	3244
S2-L1-6R	2	164	3	9	4686
S2-L1-7R	2	168	2	48	2128
S2-L1-3L	2	218	13	75	3280
S2-L1-3M	2	220	10	41	4756
S2-L1-4M	2	220	10	37	2497
S2-L1-8R	2	210	3	34	3220
S2-L1-9R	2	216	6	24	2915
S2-L1-10R	2	216	6	21	2765

	Co ppm	Dc mm/year	Cover mm
Average	3003	38	57
Standard Deviation	1044	40	10
Min	1206	2	32
Max	4756	177	77
n	27	27	66
Alfa (α)		0.94	
Beta(β)		41.11	

Copyright National Academy of Sciences. All rights reserved.

Figure A-1: Cover, Co, & Dc Distributions for Structure in Colorado

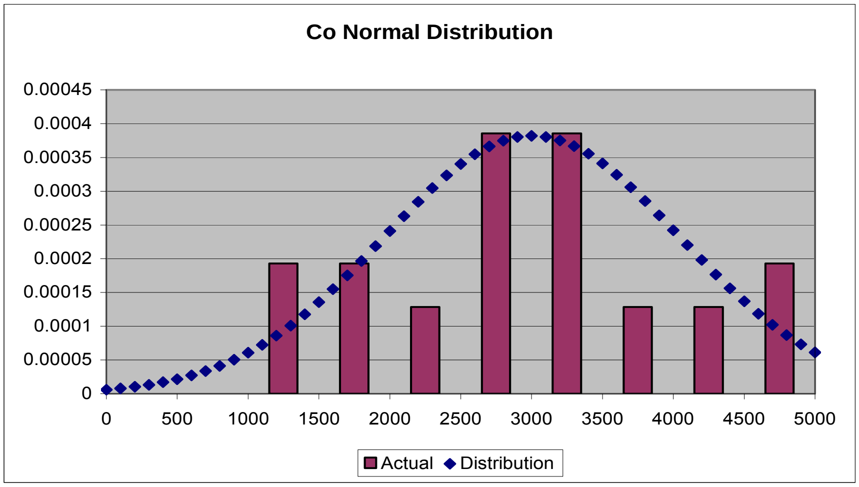

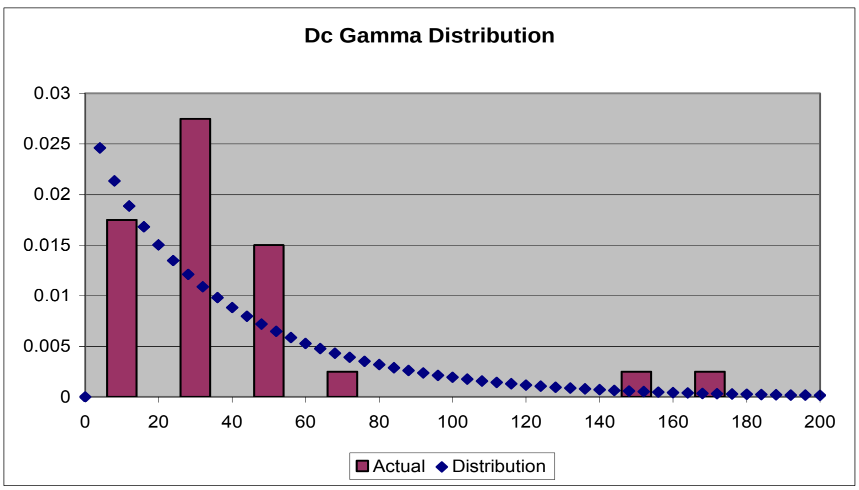

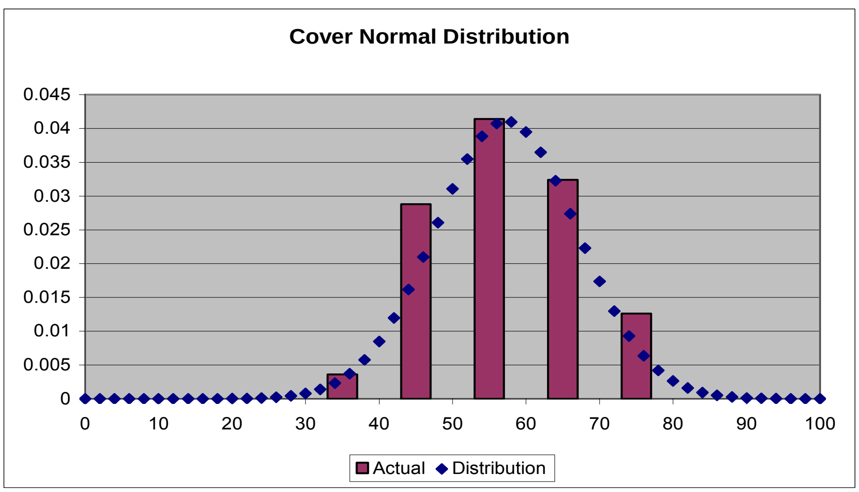

Copyright National Academy of Sciences. All rights reserved.

Table A-2: Core Information for Structure in New Mexico

Core ID	Span	X Loc feet	Y Loc feet	Dc mm/year	Co ppm
S1-L1-1R	1	3	4	12	1292
S1-L1-1M	1	9	16	12	1576
S1-L1-1L	1	10	13	9	1467
S1-L1-2M	1	10	17	8	1559
S1-L1-2R	1	11	7	6	1592
S1-L1-2L	1	16	13	21	1553
S1-L1-3R	1	18	7	8	1650
S1-L1-4R	1	22	2	23	1345
S1-L1-3L	1	25	16	13	1663
S1-L1-3M	1	26	13	12	1560
S1-L1-6R	1	28	4	40	1929
S2-L1-2R	2	31	4	12	2051
S2-L1-3R	2	35	7	19	2123
S2-L1-4R	2	39	4	35	2128
S2-L1-1L	2	39	15	8	1455
S2-L1-5R	2	46	5	11	2211
S2-L1-6R	2	50	4	21	1846
S2-L1-7R	2	53	3	39	1952
S2-L1-8R	2	58	5	85	861
S3-L1-1R	3	82	2	10	2764
S3-L1-1L	3	83	16	2	1557
S3-1L-2R	3	85	7	10	1697
S3-L1-1M	3	86	13	10	1752
S3-L1-3R	3	89	5	9	1767
S3-L1-2M	3	90	13	6	1684
S3-1L-2L	3	90	17	6	1766
S3-L1-4R	3	95	7	8	2054
S3-L1-5R	3	100	5	6	2444
S3-L1-6R	3	100	5	10	1969
S3-L1-3M	3	100	13	7	1818
S3-L1-7R	3	107	8	7	1958

	Co ppm	Dc mm/year	Cover mm
Average	1776	16	50
Standard Deviation	361	16	9
Min	861	2	28
Max	2764	85	70
n	31	31	68
Alfa (α)		0.95	
Beta(β)		16.45	

Copyright National Academy of Sciences. All rights reserved.

Figure A-2: Cover, Co, & Dc Distributions for Structure in New Mexico

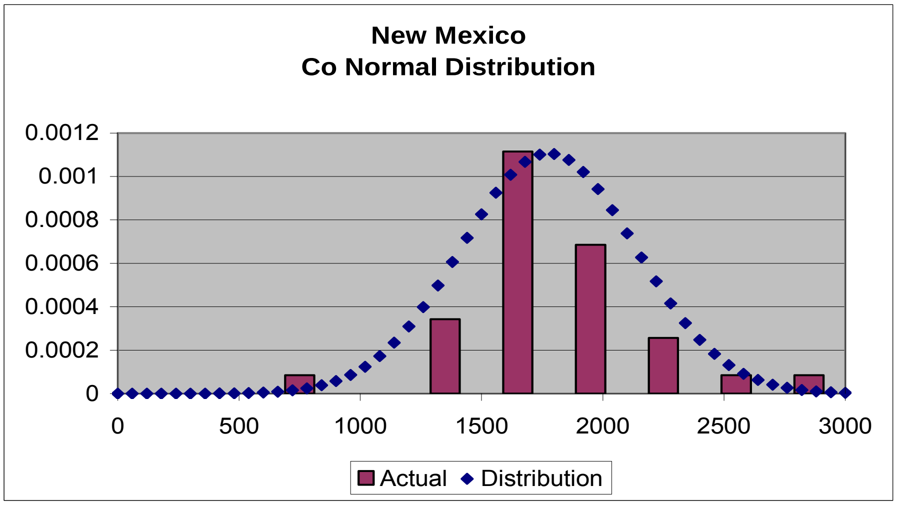

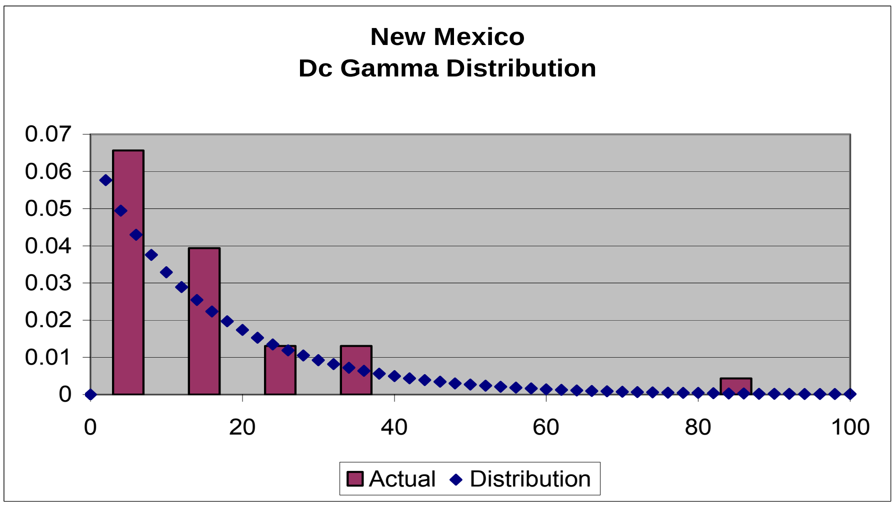

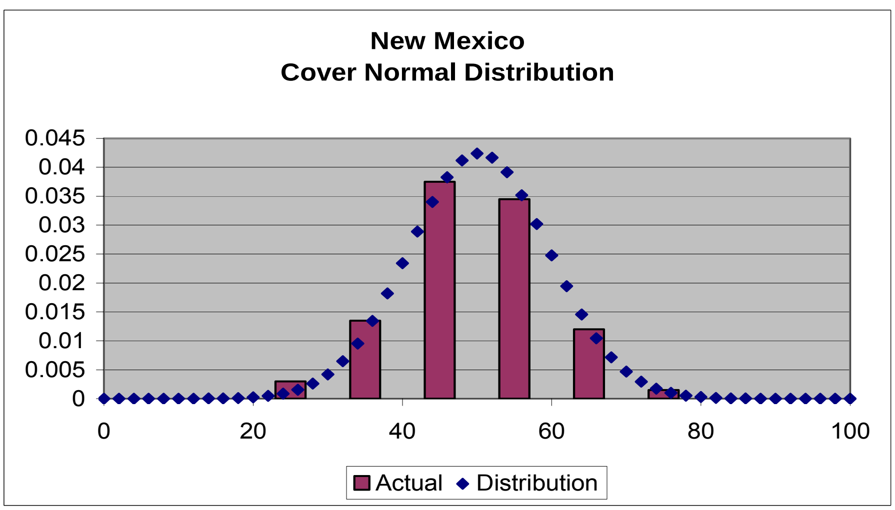

Copyright National Academy of Sciences. All rights reserved.

Table A-3: Core Information for Structure in Kentucky

Core ID	Span	X Loc feet	Y Loc feet	Dc mm/year	Co ppm
S1-L1-1R	1	16	2	16	4856
S1-L1-1M	1	20	19	13	4595
S1-L1-2R	1	32	3	28	6133
S1-L1-3R	1	40	4	22	5754
S1-L1-2M	1	43	8	33	5304
S1-L1-4R	1	45	2	25	3960
S1-L1-4RA	1			26	4848
S1-L1-4RB	1			26	4425
S1-L1-1L	1	16	21	17	3976
S2-L1-1R	2	58	2	18	4794
S2-L1-1RA	2			15	4212
S2-L1-2R	2	67	3	17	4083
S2-L1-1M	2	71	8	9	4582
S2-L1-3R	2	81	1	20	3992
S2-L1-2M	2	93	8	28	4618
S2-L1-4R	2	101	2	10	3676
S2-L1-5R	2	112	3	24	4698
S2-L1-3M	2	124	8	6	4438
S2-L1-6R	2	132	5	7	4774
S2-L1-4M	2	136	8	10	5167
S2-L1-1L	2	134	22	14	3591
S2-L1-2L	2	93	21	23	4131
S2-L1-3L	2	54	17	11	2834
S3-L1-1M	3	147	8	26	5860
S3-L1-2M	3	174	8	20	4004
S3-L1-2R	3	181	3	26	4641
S3-L1-3R	3	192	4	15	4219
S3-L1-4R	3	203	4	48	4656
S3-L1-3M	3	208	8	9	4223
S3-L1-3MA	3			17	4562
S3-L1-5R	3	216	2	10	3498
S3-L1-2L	3	215	14	10	4170
S4-L1-1R	4			18	4329
S4-L1-1M	4	234	8	13	4504
S4-1L-2R	4	243	4	18	3661
S4-L1-3R	4	255	2	12	4696
S4-L1-1L	4	254	15	11	3683

	Co ppm	Dc mm/year	Cover mm
Average	4436	18	53
Standard Deviation	667	9	7
Min	2834	6	32
Max	6133	48	69
n	37	37	70
Alfa (α)		4.49	
Beta(β)		4.03	

Copyright National Academy of Sciences. All rights reserved.

Figure A-3: Cover, Co, & Dc Distributions for Structure in Kentucky

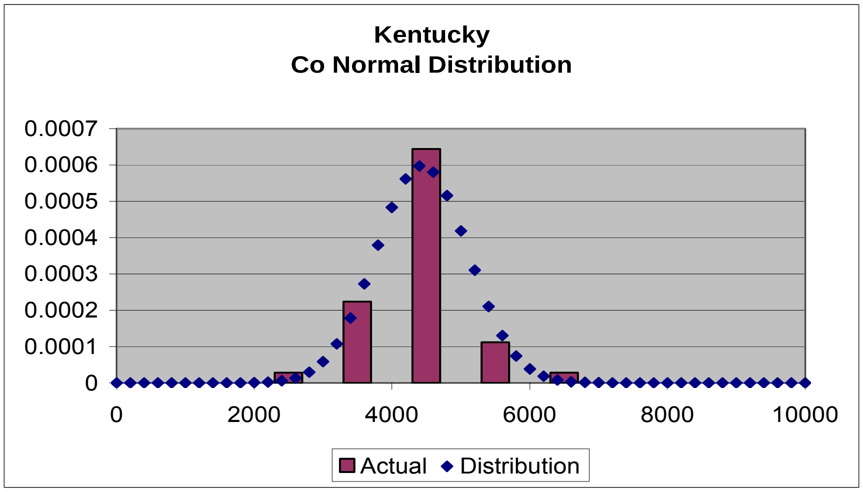

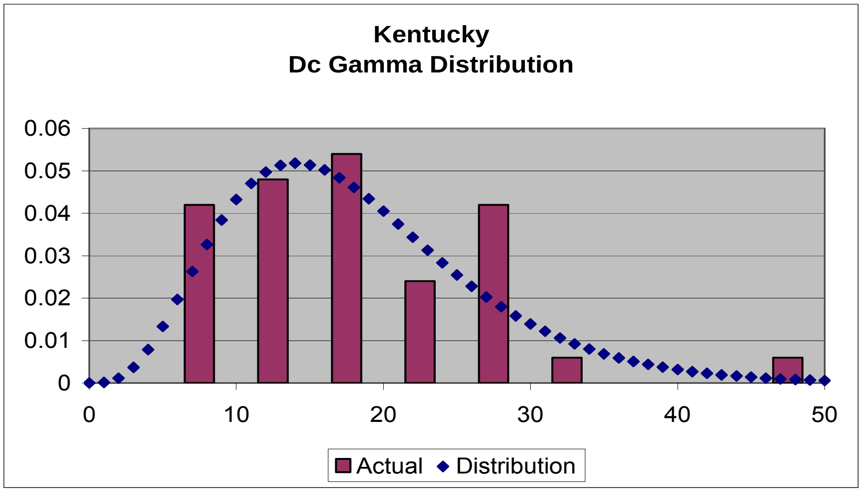

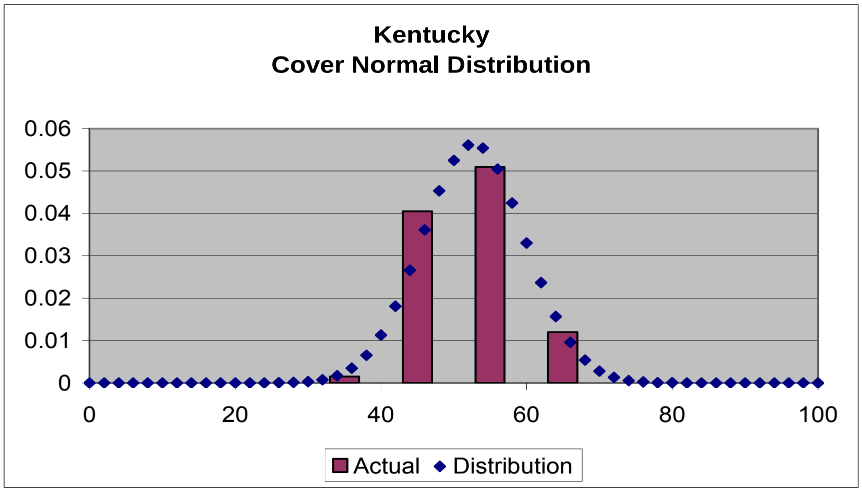

Copyright National Academy of Sciences. All rights reserved.

Table A-4: Core Information for Structure in Ohio

Core ID	Span	X Loc feet	Y Loc feet	Dc mm/year	Co ppm
S1-L1-1M	1	3	9	42	3271
S1-L1-1R	1	4	2	19	1972
S1-L1-1L	1	6	11	50	3177
S1-L1-2R	1	12	2	31	2057
S1-L1-3R	1	20	2	20	1809
S1-L1-2L	1	26	9	22	4376
S1-L1-2M	1	28	6	22	3647
S1-L1-4R	1	42	2	30	3032
S2-L1-5R	2	53	3	42	3785
S2-L1-6R	2	63	2	26	2251
S2-L1-3M	2	64	7	17	3141
S2-L1-3L	2	66	11	67	5144
S2-L1-7RA	2	76	3	36	4212
S2-L1-8R	2	83	1	27	2431
S2-L1-9R	2	90	2	41	2939
S2-L1-4L	2	92	9	50	3796
S2-L1-5L	2	99	9	9	3116
S2-L1-10R	2	110	2	27	2494
S3-L1-6L	3	112	10	14	3443
S3-L1-4M	3	113	8	10	3365
S3-L1-11R	3	113	2	34	2796
S3-L1-5M	3	121	7	58	4440
S3-L1-7L	3	122	11	31	4879
S3-L1-12R	3	123	2	34	2840
S3-L1-13R	3	134	2	44	2433
S3-L1-6M	3	135	8	34	5436
S3-L1-8L	3	136	11	48	5896
S3-L1-14R	3	145	3	16	3310
S3-L1-15R	3	153	3	56	2997
S4-L1-16R	4	164	2	31	2135
S4-L1-9L	4	166	10	28	4024
S4-L1-7M	4	168	5	45	4117
S4-L1-8M	4	181	6	50	4021
S4-L1-17R	4	190	2	53	3169
S2-L1-7RB	2			35	4368

	Co ppm	Dc mm/year	Cover mm
Average	3438	34	56
Standard Deviation	1004	14	8
Min	1809	9	37
Max	5896	67	77
n	35	35	68
Alfa (α)		5.66	
Beta(β)		6.07	

Copyright National Academy of Sciences. All rights reserved.

Figure A-4: Cover, Co, & Dc Distributions for Structure in Ohio

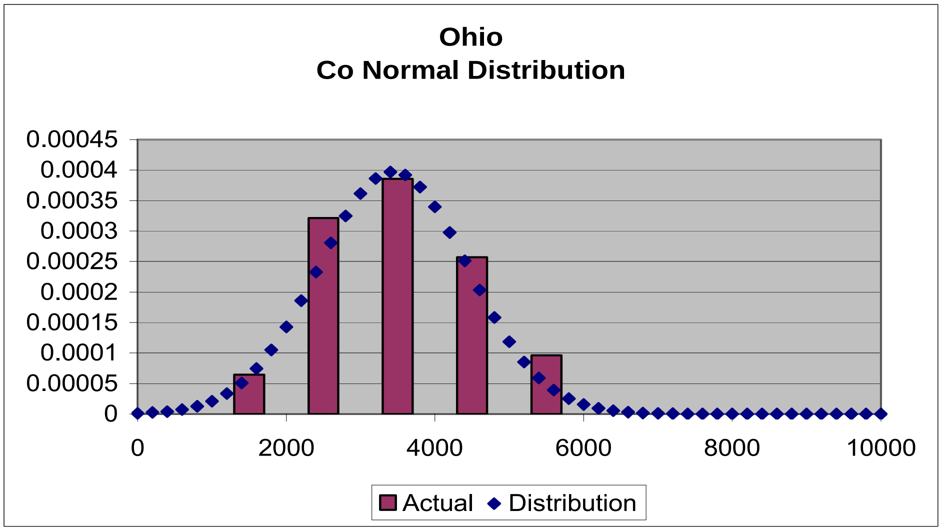

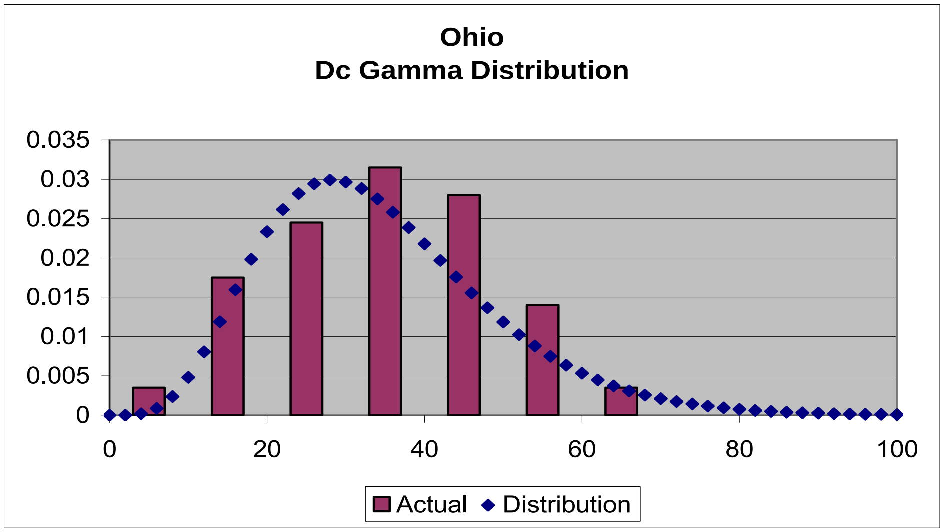

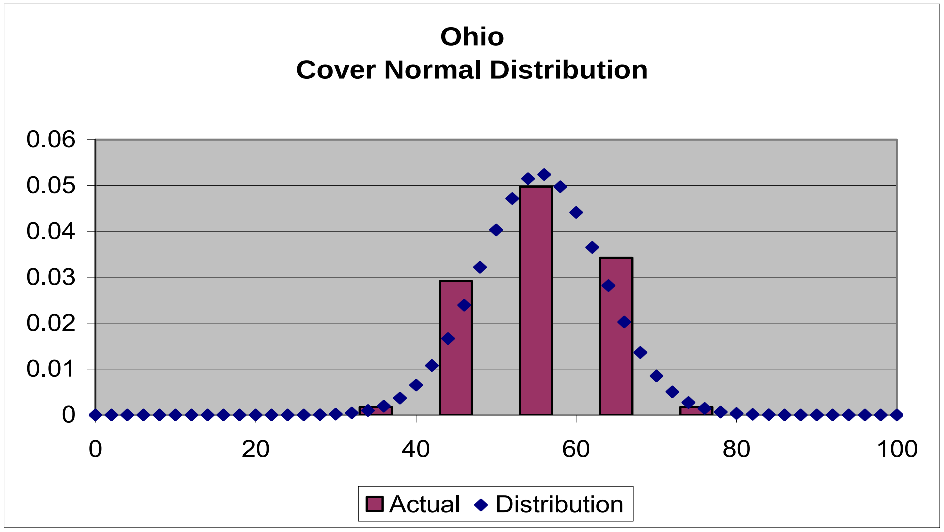

Copyright National Academy of Sciences. All rights reserved.

Table A-5: Core Information for Structure in Maryland

Core ID	Span	X Loc feet	Y Loc feet	Dc mm/year	Co ppm
S1-L1-3L	1	14	8	140	3350
S1-L1-4L	1	15	9	162	4762
S1-L1-1R	1	19	1	1	2734
S1-L1-2L	1	32	8	118	4254
S1-L1-5L	1	32	8	66	5291
S2-L1-1L	2	75	7	20	5756
S2-L1-11L	2	107	7	269	3482
S3-L1-1L	3	155	9	28	5063
S3-L1-4L	3	157	7	120	4827
S3-L1-3L	3	158	9	18	6076
S3-L1-5L	3	166	8	38	4318
S3-L1-7L	3	191	7	48	4835
S3-L1-9L	3	199	8	79	4743
S3-L1-10L	3	203	7	44	6465
S3-L1-11L	3	207	8	19	5484
S3-L1-12L	3	207	8	43	4841
S3-L1-14L	3	227	7	35	4656
S3-L1-15L	3	231	8	43	4966

	Co ppm	Dc mm/year	Cover mm
Average	4772	72	64
Standard Deviation	932	67	5
Min	2734	1	56
Max	6465	269	75
n	18	18	31
Alfa (α)		1.14	
Beta(β)		62.98	

Copyright National Academy of Sciences. All rights reserved.

Figure A-5: Cover, Co, & Dc Distributions for Structure in Maryland

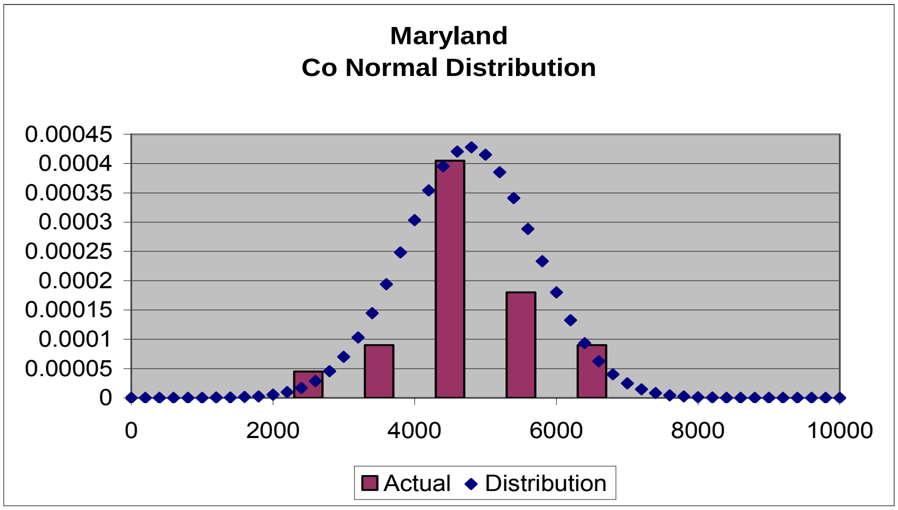

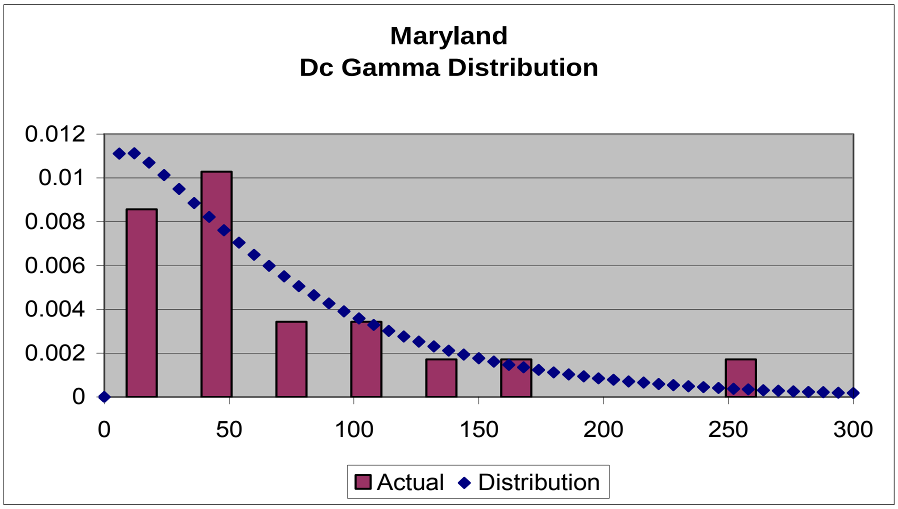

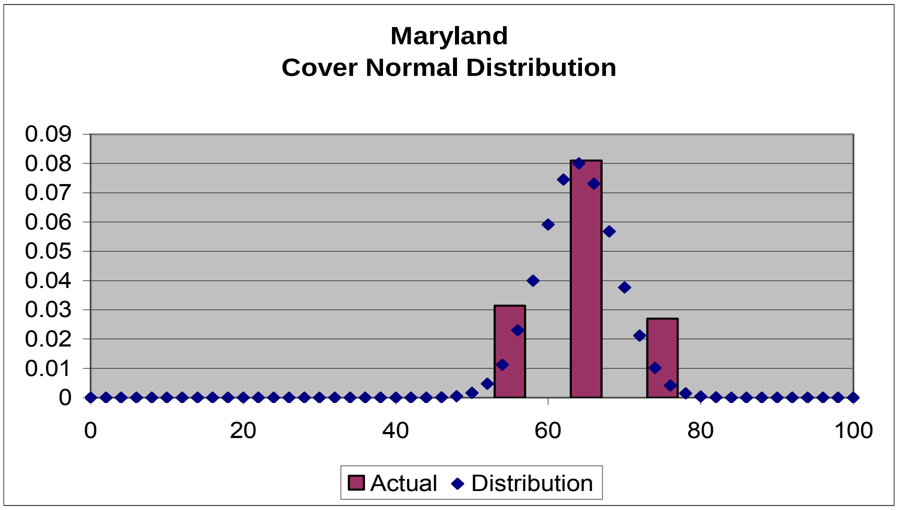

Copyright National Academy of Sciences. All rights reserved.

Table A-6: Summary of Corrosion Rate Measurements

States	Trip	N	Min	Max	Average	Standard Deviation
CA	1	8	0.001	0.062	0.013	0.020
	2	10	0.041	0.260	0.101	0.066
CO	1	11	0.126	11.024	2.573	3.429
	2					
NM	1	25	0.001	0.534	0.083	0.134
	2	4	0.003	0.310	0.118	0.143
KY	1	30	0.005	0.867	0.187	0.214
	2	30	0.010	0.593	0.172	0.168
OH	1	27	0.005	0.843	0.162	0.173
	2	15	0.023	0.694	0.316	0.234
MD	1	27	3.910	54.195	15.871	11.709
	2	7	0.146	0.865	0.343	0.241

Copyright National Academy of Sciences. All rights reserved.

Figure A-6: Half-cell Potential Mapping for Bridge Deck of Structure located in California

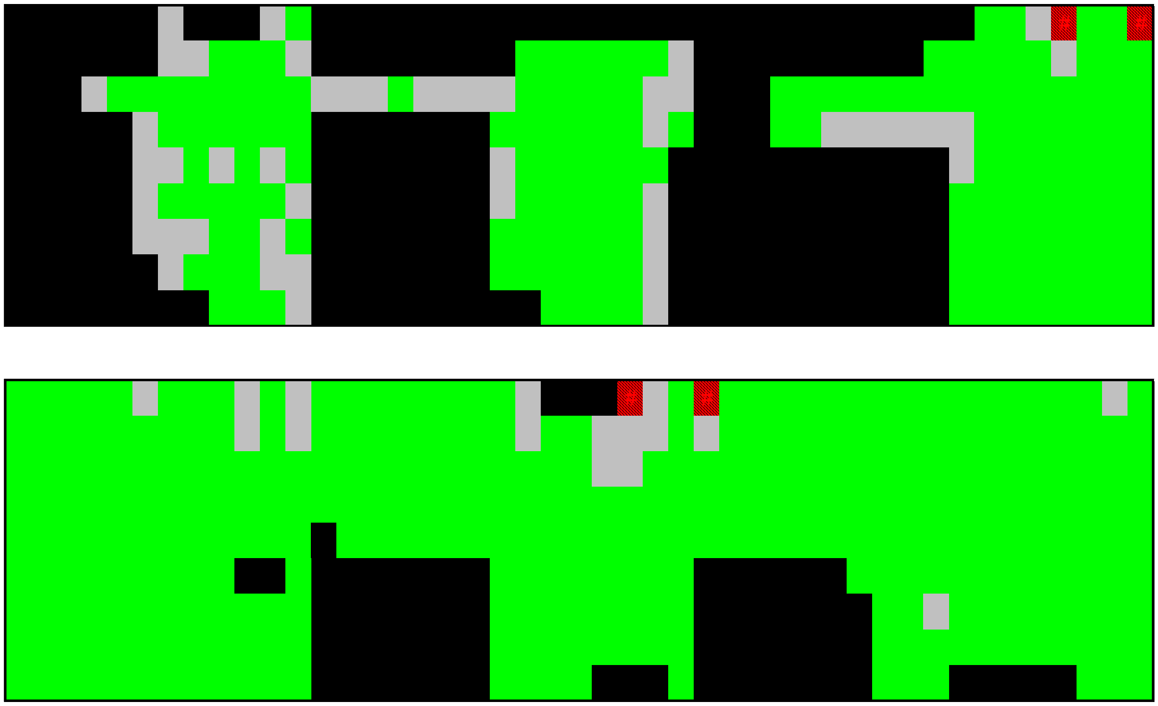

Note: All potential measured with respect to copper-copper sulfate reference electrode

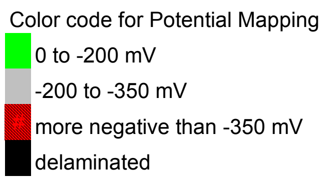

Copyright National Academy of Sciences. All rights reserved.

Figure A-7: Half-cell Potential Mapping for Bridge Deck of Structure located in New Mexico

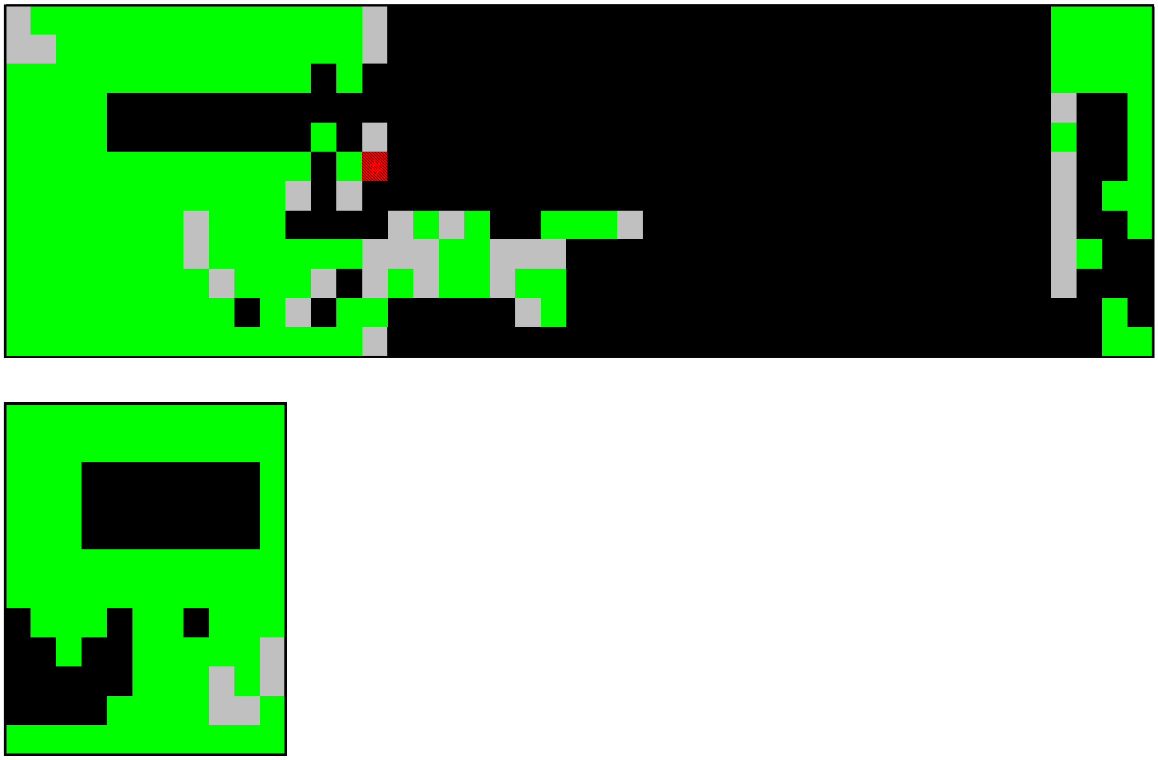

Note: All potential measured with respect to copper-copper sulfate reference electrode
Color code for Potential Mapping
0 to -200 mV
-200 to -350 mV
more negative than -350 mV
delaminated

Copyright National Academy of Sciences. All rights reserved.

Figure A-8: Half-cell Potential Mapping for Bridge Deck of Structure located in Kentucky

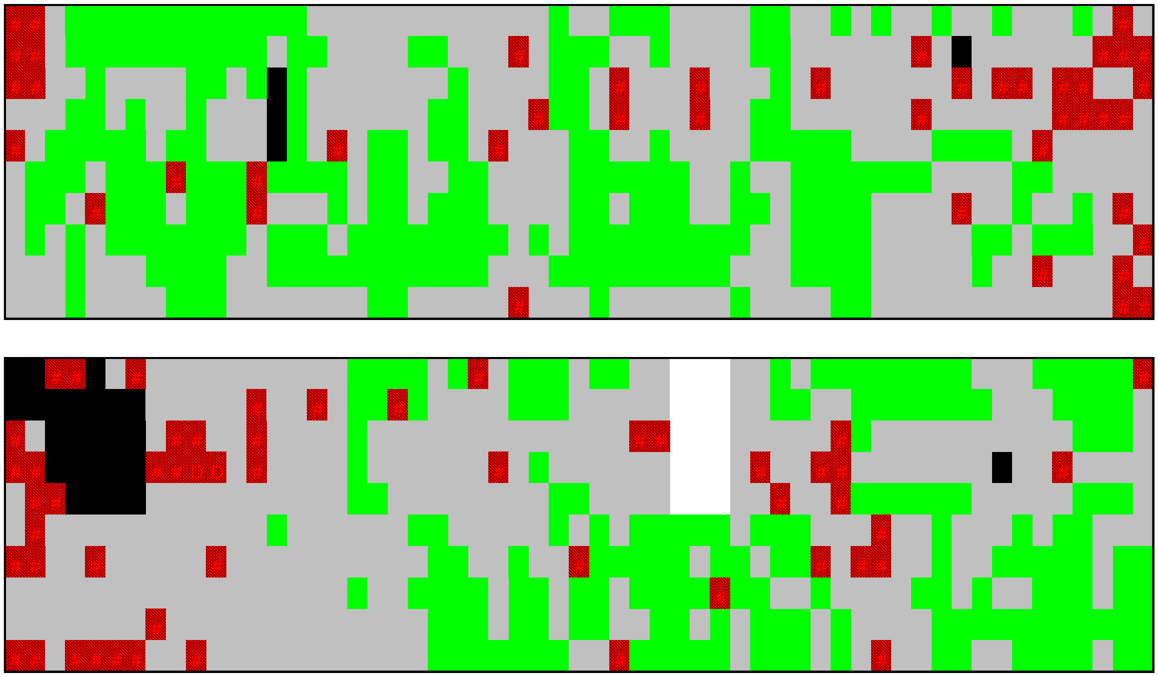

Note: All potential measured with respect to copper-copper sulfate reference electrode
Color code for Potential Mapping
0 to -200 mV
-200 to -350 mV
more negative than -350 mV
delaminated

Copyright National Academy of Sciences. All rights reserved.

Figure A-9: Half-cell Potential Mapping for Bridge Deck of Structure located in Ohio

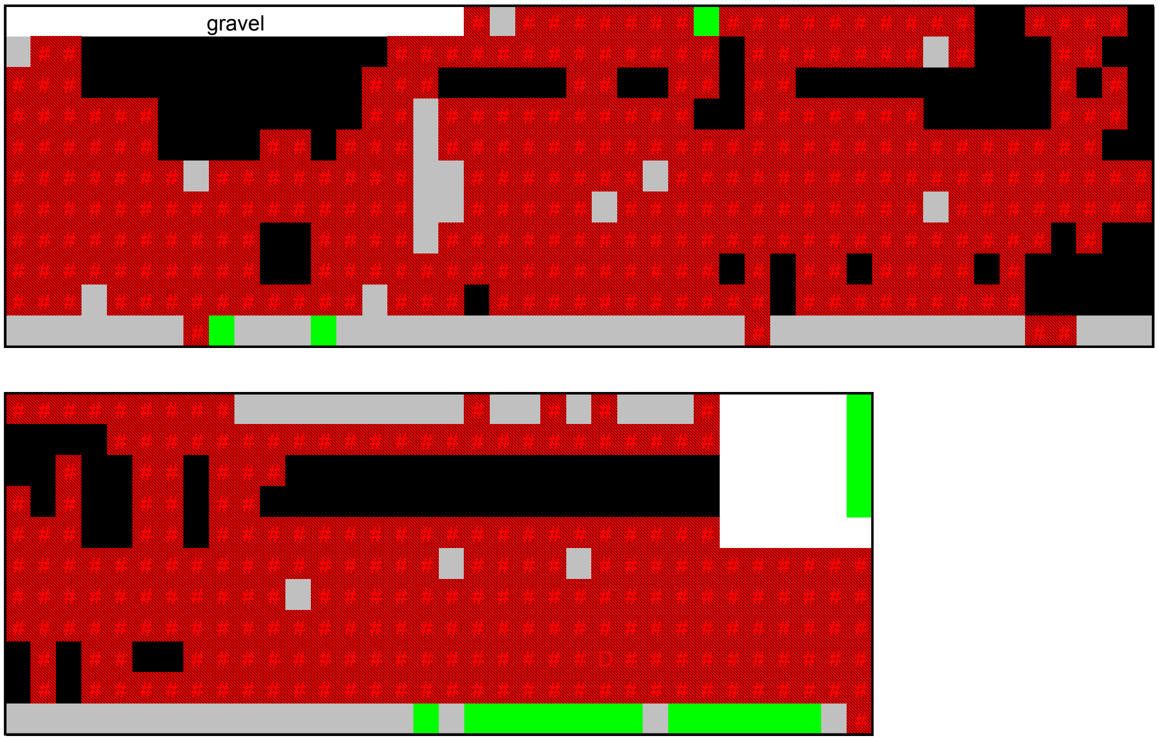

Note: All potential measured with respect to copper-copper sulfate reference electrode
Color code for Potential Mapping
0 to -200 mV
-200 to -350 mV
more negative than -350 mV
delaminated

Copyright National Academy of Sciences. All rights reserved.

Figure A-10: Half-cell Potential Mapping for Bridge Deck of Structure located in Maryland

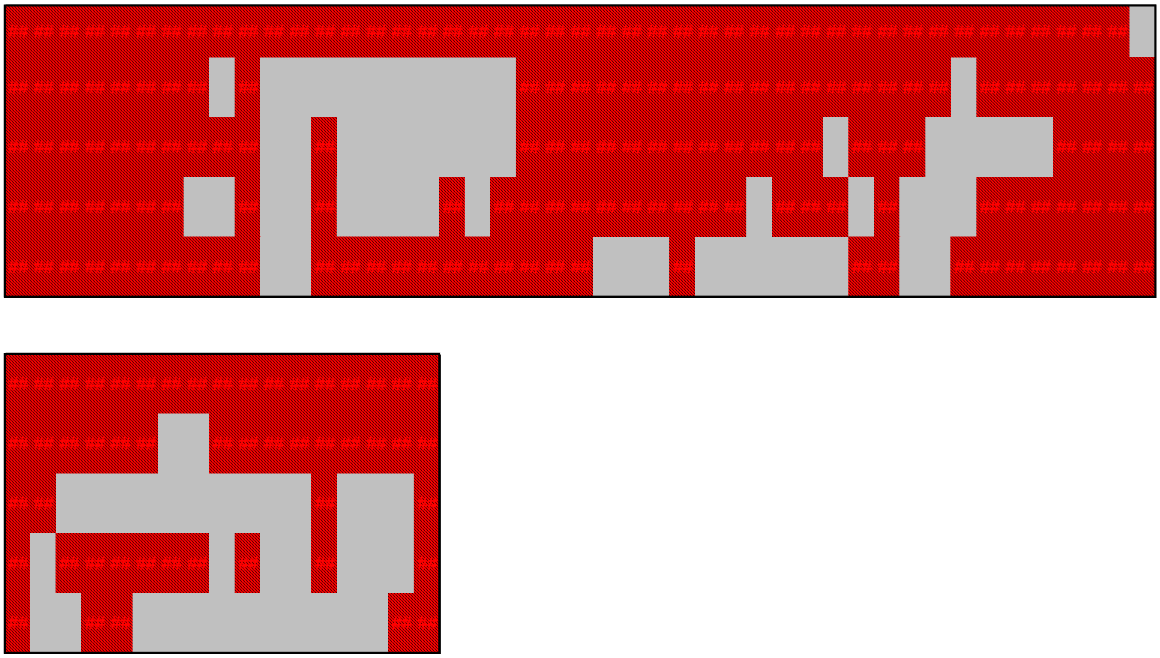

Note: All potential measured with respect to copper-copper sulfate reference electrode

Color code for Potential Mapping

0 to -200 mV

-200 to -350 mV

more negative than -350 mV

delaminated

Copyright National Academy of Sciences. All rights reserved.

Figure A-11: Model Output for the full set of cores

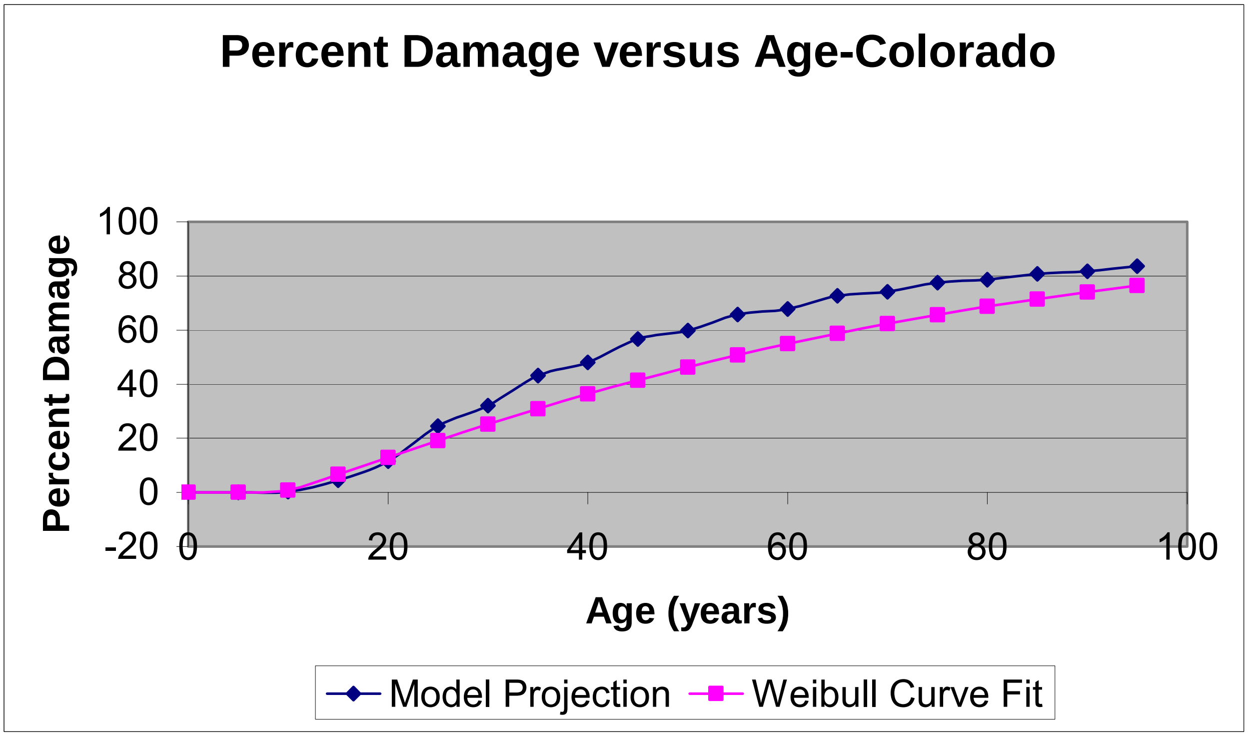

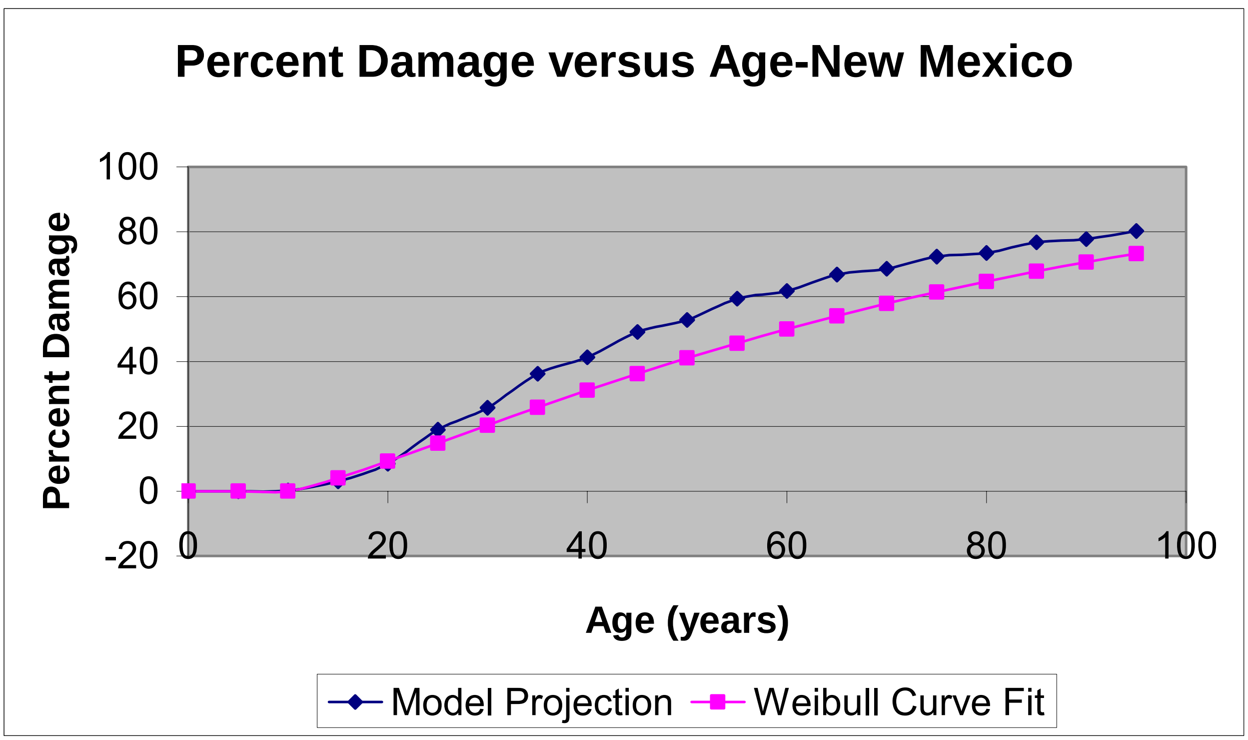

Copyright National Academy of Sciences. All rights reserved.

Figure A-11: Model Output for the full set of cores (Continued)

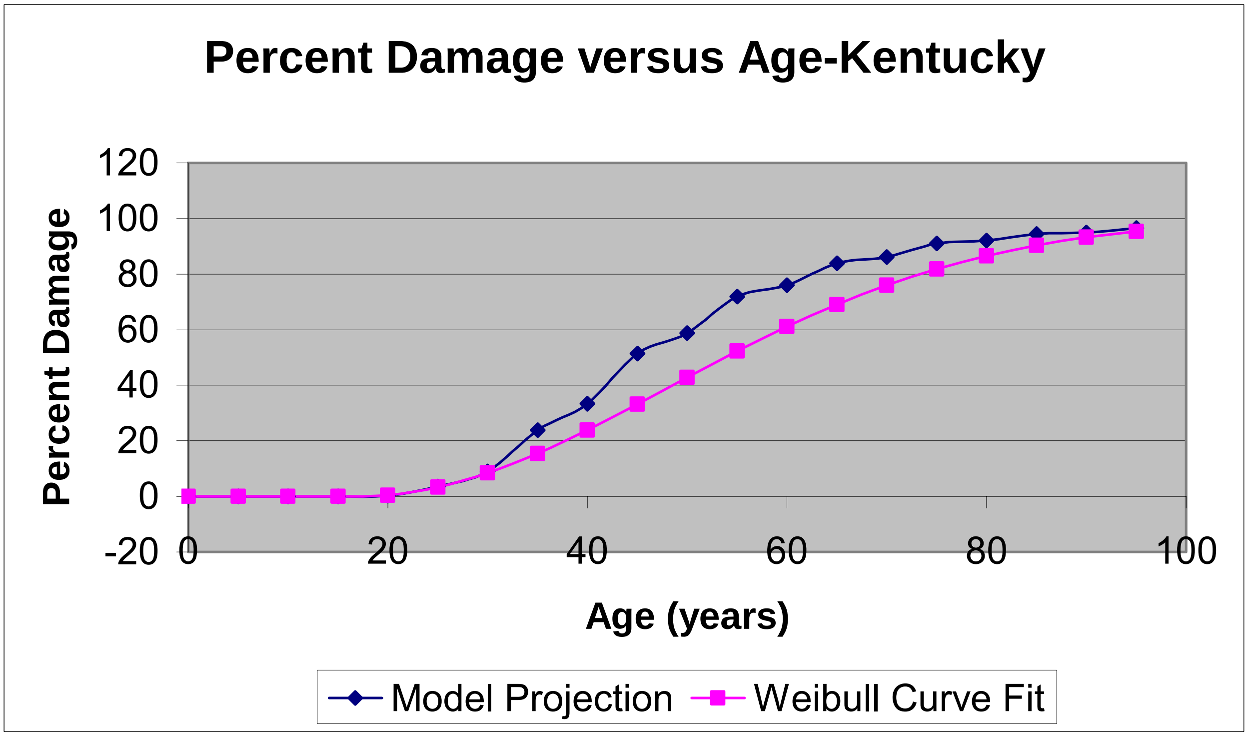

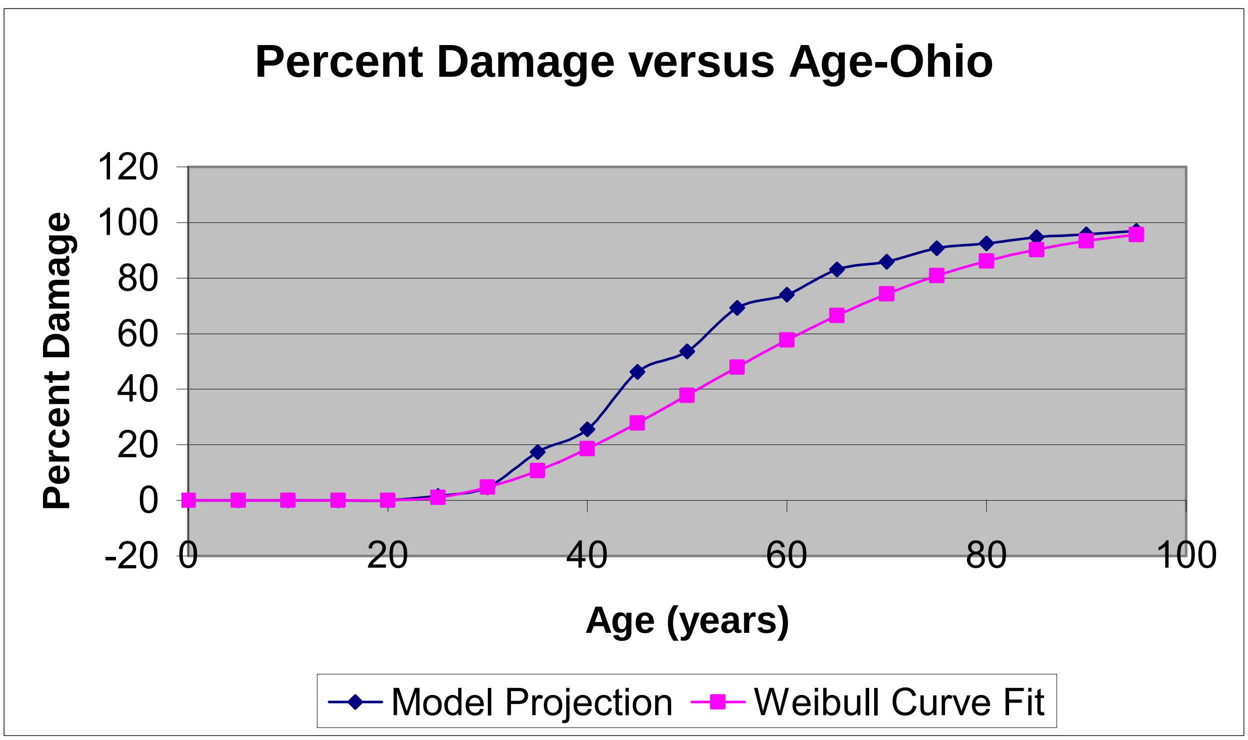

Copyright National Academy of Sciences. All rights reserved.

Figure A-11: Model Output for the full set of cores (Continued)

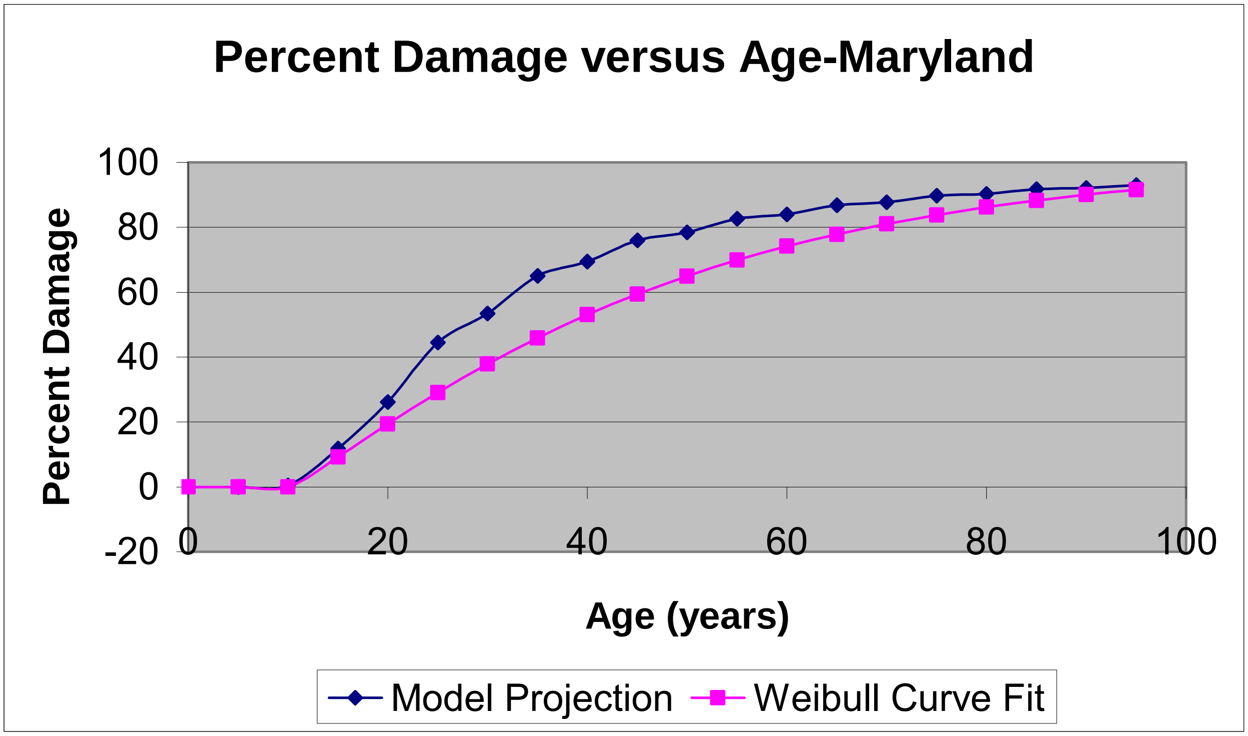

Copyright National Academy of Sciences. All rights reserved.